NMT COMMUNICATIONS

special

May 2023 Vol. 1 No.3

Technical features

- **Live/real-time**
- **Dynamic transfer process**
- No marking required
- 3D measurement
- Controllable external environment
- Unlimited material size
- Reveal size and direction
- Simultaneous detection of multi-ion molecules
- Artificial intelligence automatic detection

NMT International Alliance Publish
ISSN 2834-5363

Scientific research junction

Scientific research combination point of biomedicine and non-invasive micro-test technology (NMT)

I Summary

1. Real-time transmembrane transport processes of Ca^{2+}, K^{+}, Na^{+}, Cl^{-}, O_2 were quantitatively detected using living brain slices, spinal cord and neurons as materials;

2. Using muscle tissue and muscle cells as materials, the real-time transmembrane transport processes of $Ca^{2+}$and K^{+}were quantitatively detected;

3. The real-time transmembrane transport process of $H^{+}$and Cl - was quantitatively detected using intestinal tissue and cells as materials;

4. The real-time transmembrane transport processes of H^{+}, Ca^{2+} and H_2O_2 were quantitatively detected using tumor tissues and cells as materials.

II Application cases

1. *Nat Cell Biol*： NMT found that the increase of O_2 consumption rate of neuron mitochondria provides direct evidence for Bcl_2 family to improve neuron metabolism

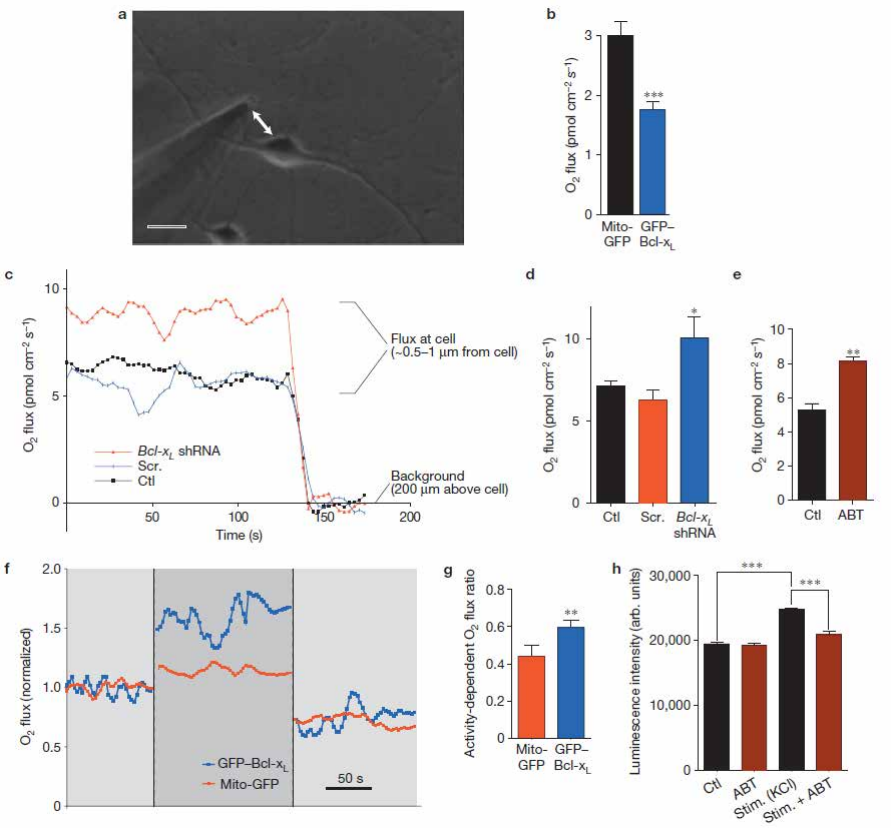

Note: Anti-apoptotic Bc_{l2} family proteins (such as Bcl-x_L) protect cells from death by isolating apoptotic molecules, but also contribute to normal neuronal function. Previous work described the increase of mitochondrial biomass in neurons overexpressing Bcl-x_L. If the increase of mitochondrial biomass is the only reason for the increase of ATP level, the cells expressing Bcl-x_L are expected to increase oxygen uptake. To verify this, NMT was used to measure the oxygen uptake of individual neurons. Contrary to expectations, the O_2 flow rate of neurons overexpressing Bcl-x_L was lower than that of neurons transfected with mito-GFP (b), indicating that neurons overexpressing Bcl-x_L were more effective in combining ATP production with O_2 absorption. Endogenous Bcl-xL has a similar effect because shRNA-mediated consumption (c, d) or pharmacological inhibition of Bcl-xL activity (e) increases the O_2 flow rate of neurons. These data indicate that the consumption or inhibition of Bcl-x_L uncouples ATP production with O_2 uptake.

2. *J Biol Eng* Purdue University: Mammalian spinal cord injury induces Ca^{2+} to significantly absorb and interfere with Ca^{2+} mediated ionic current, which may be one of the means to alleviate secondary injury

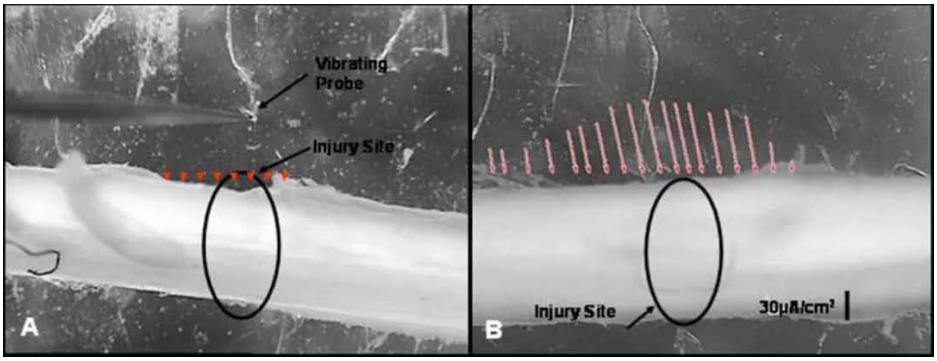

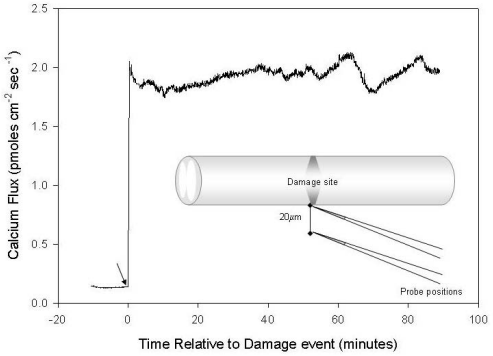

Note: After the nervous system is damaged, a series of physical, physiological and anatomical events immediately lead to the functional collapse of neurons and often death. This progression of the injury process is called "secondary injury". The study investigated the most neglected and earliest components of secondary injury. Large biological currents immediately enter the injured guinea pig spinal cord cells and tissues. The driving force behind these currents is the potential difference of adjacent intact cell membranes. The huge biological current crosses the injured part of the mammalian spinal cord. The endogenous current decreases with time and the distance from the injured site, but ultimately maintains a low but stable value. During this process, it is very important that the Ca^{2+} influx at the injured site lasts for more than 1h. Strangely, the injury current entering the ventral side of the spinal cord may be 10 times higher than the injury current entering the dorsal surface, and compared with the spinal cord transection, there is little difference in the magnitude of the current related to the crush injury. The research shows that the huge bioelectric current is partly carried by free calcium, which is the main initiator of the secondary injury process, and will cause greater damage after damaging the vulnerable cell membrane adjacent to the injury site.

Scientific research combination point of heavy metal and non-invasive micro-test technology (NMT)

I Summary

1. Phenotype study

1) Quantitative detection of the real-time absorption rate of Cd^{2+}/Cu^{2+}/Pb^{2+}in the environment by living samples such as roots, leaves, algae, biofilms, bacteria and fungi

2) Quantitatively detect the transport rate of Cd^{2+}/Cu^{2+}/Pb^{2+} in living plants, including root xylem loading, stem xylem vessel transport, mesophyll absorption, vacuole partition) and other processes

3) Quantitative determination of the changes in the absorption rate of Mg^{2+}, K^{+}, Ca^{2+} and other elements by animal and plant tissues and cells in the presence of heavy metals, and study the process of element imbalance caused by heavy metals

4) Quantitative determination of Cd^{2+}/Cu^{2+}/Pb^{2+} concentration at different positions inside and outside the living sample

2. Mechanism

1) Ca^{2+} signal

With the absorption and transport rate of Cd^{2+}/Cu^{2+}/Pb^{2+} as the foothold, from Ca^{2+} signal to promote ROS production, ROS to regulate the plasma membrane Cd^{2+}/Cu^{2+}/Pb^{2+} transport carrier, supplemented by Ca^{2+} channel inhibitor, RBOH inhibitor, ROS scavenger, etc., verify how Ca^{2+} participates in the regulation of heavy metal absorption and transport, and verify the functions of Nramp, HMA, IRT, ZIP, Ctr, Fet4, etc

2) Secreting H^{+} regulating rhizosphere pH

Quantitative detection of root real-time H^{+} secretion rate and root surface pH under heavy metal stress, characterizing the ability of plants to cope with stress by promoting nutrient absorption and excretion of heavy metal ions under heavy metal stress

3) O_2 uptake/secretion regulates the redox potential in the rhizosphere

II Application cases

1. *J Adv Res* Damage micro-measurement technology found that NAT2 promoted Cd uptake in barley, providing evidence for NAT as a potential heavy metal bioremediation gene

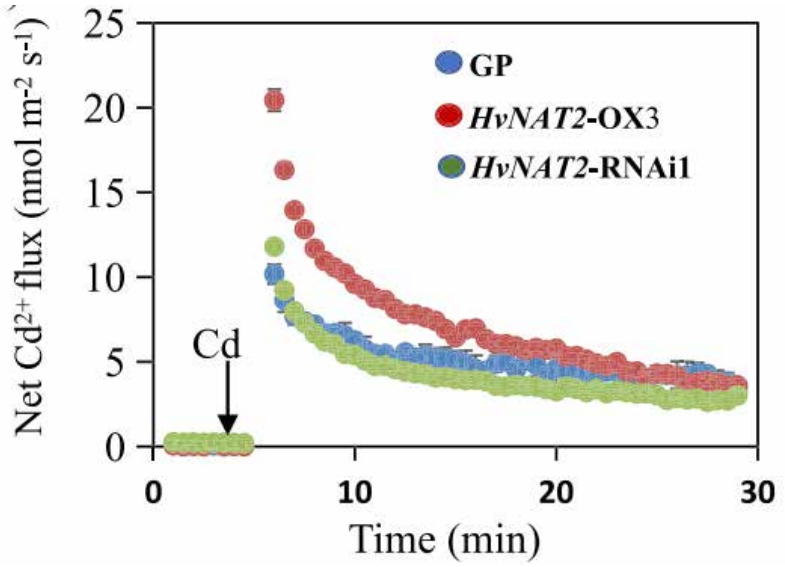

Note: In order to study the effect of different genotypes on the Cd^{2+} flow rate of root epidermal cells, the dynamic change of Cd^{2+} flow rate of root epidermal cells after $CdCl_2$ treatment was detected by non-invasive micro-measurement technology. The result shows that adding 10 μ M $CdCl_2$ caused the rapid influx of Cd^{2+} in plant epidermal cells; Compared with GP control, *HvNAT2-OX3* plants had the highest Cd^{2+} transport velocity; The total and average Cd^{2+} flow rates of *HvNAT2-OX3* plants were significantly higher than those of GP (31% and 39% respectively), while the steady-state Cd^{2+} flow rates of *HvNAT2*-RNAi1 roots were significantly reduced by 23%.

2. *Environ Pollut* Mechanism of Si-dependent Cd/Cu/Pb tolerance of diatoms

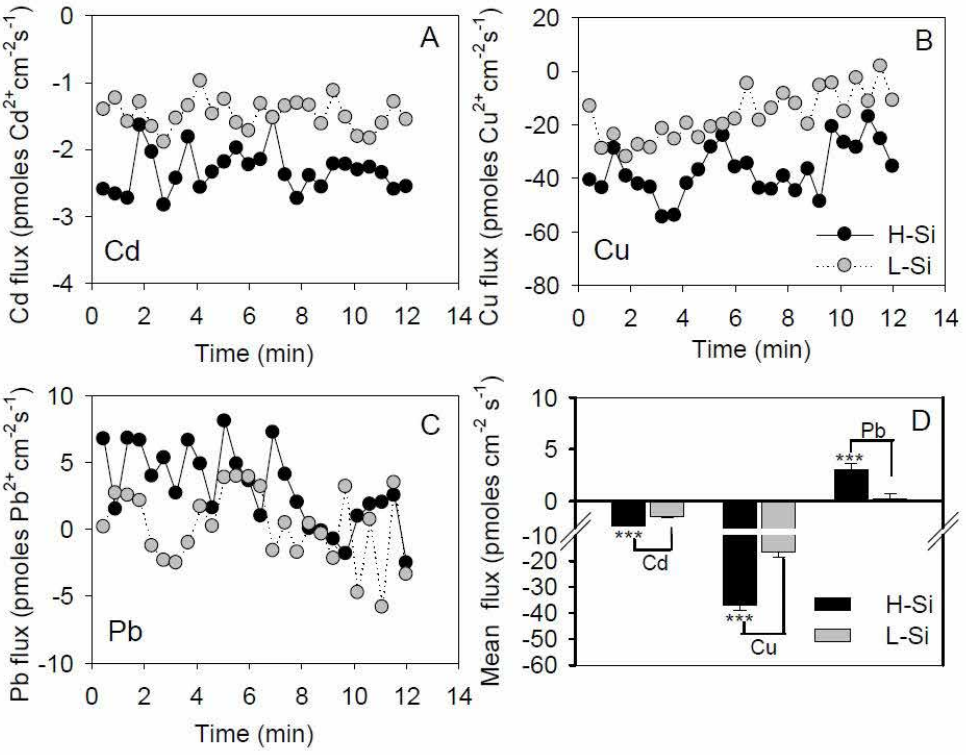

Note: The flow rate of Cd^{2+} varies between - 2.84 and - 0.98, the metal flow rate of Cu^{2+} varies between - 54.66 and 1.77, and the metal flow rate of Pb^{2+} varies between - 5.84 and 8.07. The negative values of Cd^{2+} and Cu^{2+} indicate that the absorption of these ions exceeds their elimination. However, for Pb^{2+} , the values of L-Si and H-Si cells are positive, indicating that the elimination of Pb^{2+} is faster than the absorption during the initial contact with metal. The absorption rate of Cd^{2+} and Cu^{2+} in H-Si cells was faster than that in L-Si cells ($p<0.05$). On the contrary, the Pb^{2+} outflow of H-Si cells was significantly higher than that of L-Si cells ($p<0.05$). It shows that the silicon rich cells have higher metal adsorption and inflow rate than the silicon deficient cells.

Scientific research combination point of nutrient elements and non-invasive micro-test technology (NMT)

I Summary

1. Quantitative detection of root, leaf, algae, microorganism and other living samples, real-time absorption rate of $NH_4^+/NO_3^-/K^+/Mg^{2+}$ in the internal/environmental environment, and verification of NRT, CLC, SLAC, AMT, MEP, HAK, HKT, MGT, MHX and other functions

2. Quantitative detection of real-time transport rate of $NH_4^+/NO_3^-/K^+/Mg^{2+}$ in living plants, including root xylem loading, stem xylem vessel transport, mesophyll absorption and other processes

3. Quantitatively detect the dynamic change (H^+ transport rate) and pH of H^+ in the process of $NH_4^+/NO_3^-/K^+/Mg^{2+}$ /Fe^{2+}absorption and transport, and reveal the mechanism of OSA and AHA participating in nutrient element absorption and transport

4. Quantitatively detect the real-time rate and direction of vacuolar transport of $NH_4^+/NO_3^-/K^+$, study the intracellular nitrogen and potassium homeostasis, and verify the functions of NHX, CLC, etc

5. Quantitative detection of the rate of real-time NH_4^+/NO_3 excretion by living roots under high NH_4^+/high NO_3 stress

II Application cases

1. *Plant Physiol* NMT found that anion channel regulators regulate nitrate channels and promote nitrate efflux to alleviate plant ammonium toxicity

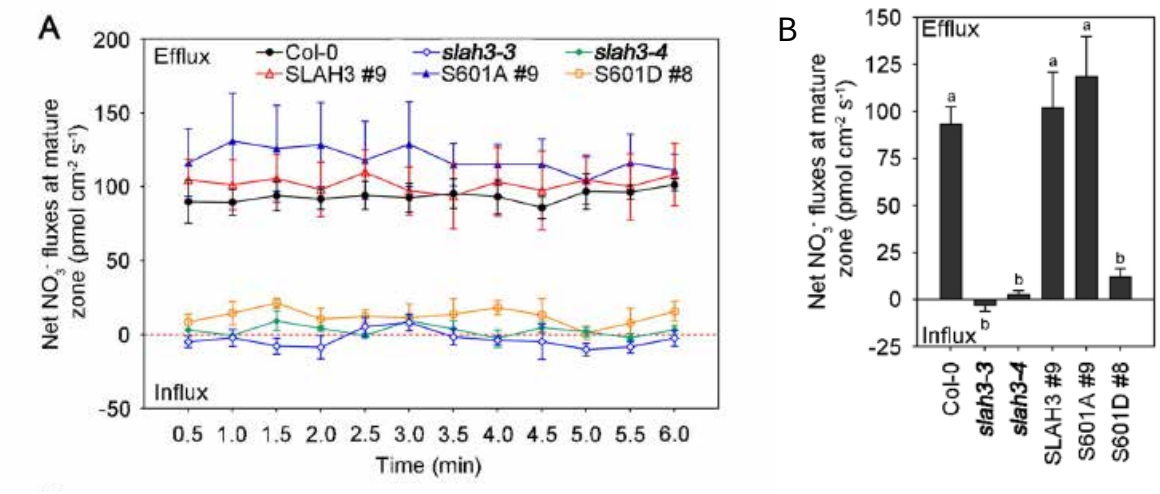

Figure 1

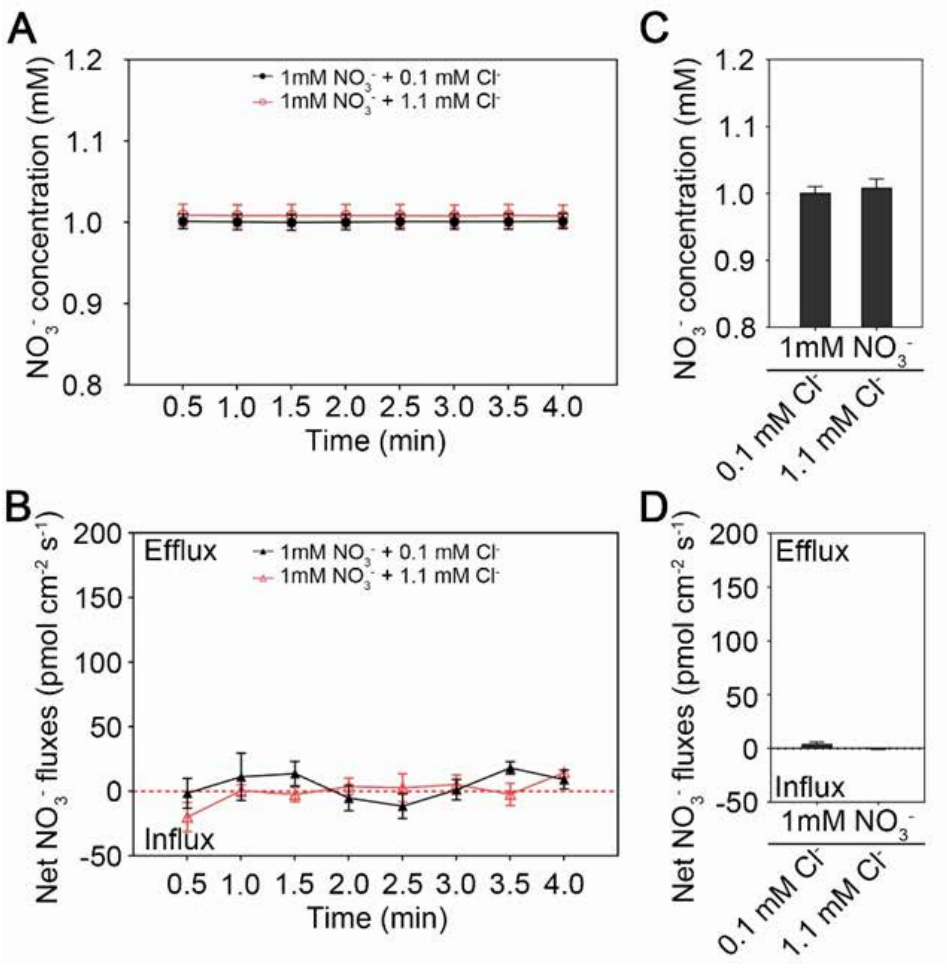

Figure 2

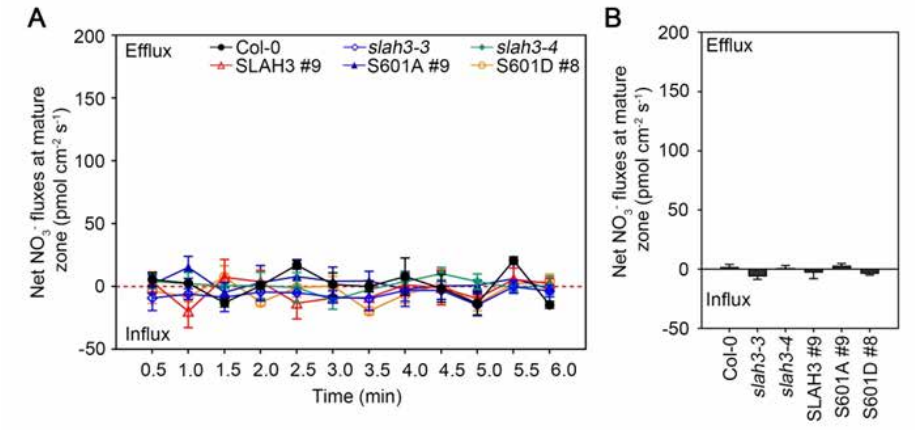

Figure 3

Note: This study detected the NO_3 net flow rate in the mature zone near the root tip (Figure. 1A, Figure. 3A). Col-0, *slah3-3*, *slah3-4* seedlings and all complementary strains were grown on 1/2 MS medium for 8 days and then transferred to high NH_4^+ /low pH conditions (1 mM NO_3^-, 10 mM NH_4^+ , pH 4.5) or non-high NH_4^+ /low pH conditions (1 mM NO_3 -, 1 mM NH_4^+ , pH 5.7) for 2 hours. NO_3 flow rate from plant roots was detected within 6 min (Figure. 1B, Figure. 3B). Under high NH_4^+ /low pH stress, the average NO_3 efflux rate of Col-0 was about 93, and the average NO3 efflux rate of slah3 mutant was about 0. The complementary lines *SLAH3* and *SLAH3 S601A* under the background of *slah3-4* showed nitrate efflux similar to that of Col-0. In contrast, the nitrate efflux of the complementary line SLAH3 S601D under the background of *slah3-4* is similar to that of the slah3 mutant (Figure. 1B). In addition, under non-high NH_4^+ /low pH stress, nitrate efflux of all plants is similar, and the average value of NO3 efflux rate is around 0 (Figure 3). These results indicate that S601 of *SLAH3* plays an important role in regulating nitrate efflux under high NH_4^+ / low pH stress.

2. *Curr Biol* NMT provides a basis for revealing the regulatory effect of magnesium on carbon and nitrogen nutrient exchange in soybean nodules

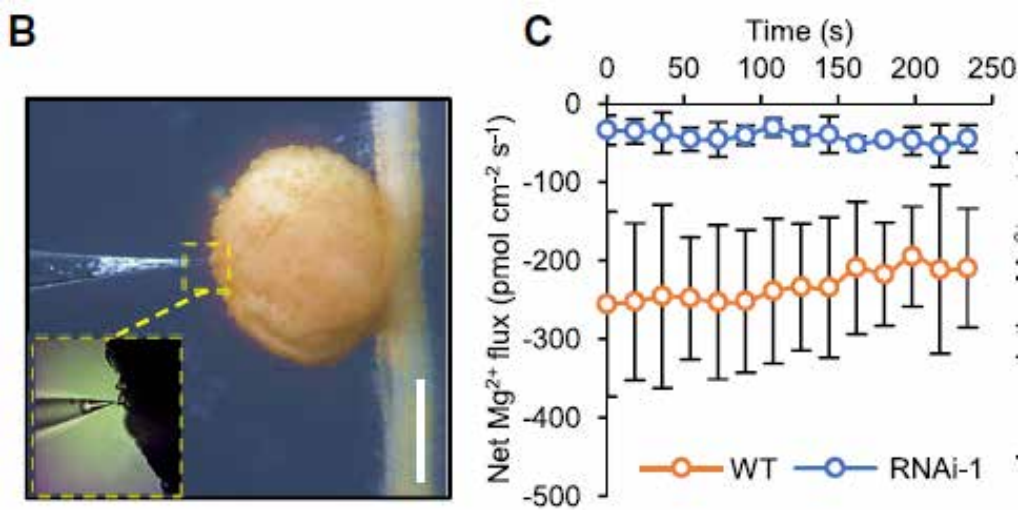

Note: The use of NMT to monitor the net flow rate of magnesium in real time (B) shows that by knocking out the expression of GmMGT4 and 5, the input amount of magnesium in nodules is significantly reduced (C), which leads to a significant reduction in the cumulative amount of magnesium in nodules. It provides basis for the regulation of carbon - nitrogen nutrient exchange in soybean nodules.

Saline-alkali stress and non-invasive micro-test technology (NMT) scientific research junction

I Summary

1. Phenotype study

1) Quantitative detection of the Na^+ excretion/absorption rate of the sample, direct characterization of the activity of Na-H reverse transporter and Na-H exchanger, and verification of SOS1, NHX1 and other functions

2) Quantitatively detect the rate of K^+ loss of samples and directly characterize their comprehensive salt tolerance and K^+ retention ability

3) Quantitative detection of Na^+ and K^+ concentrations at different positions inside and outside living samples

2. Mechanism research

1) Guarantee K^+ mechanism

A. Outward K^+ channel (GORK) salt tolerance and K^+ contribution rate

Quantitative detection of H^+ excretion rate under salt stress, combined with its K^+ retention capacity, to determine whether the K^+ retention mechanism of samples with strong salt tolerance/K^+ retention capacity is through active PM H^+ - ATPase H^+ excretion, promoting plasma membrane repolarization under salt stress, closing GORK, thus achieving the K^+ retention effect

B. Non-selective cation channel (NSCC) salt tolerance and K^+ contribution rate

Taking the K^+ efflux rate as the foothold, from the key signal ROS of NSCC activation and the pathway of ROS intracellular and extracellular production, using RBOHs mutants, RBOH inhibitors, intracellular ROS scavengers, etc., to verify whether the K^+ preservation is achieved by regulating NSCC and its regulatory mechanism

2) Proton pump H^+ - ATPase

Detect the real-time H+excretion rate under salt stress, and use the most direct indicator to quantitatively characterize the extent of the increase of H^+ - ATPase activity under salt stress

3) Ca^{2+} signal transduction

Taking the rate of Na^+ excretion/absorption and the rate of K^+ loss as the foothold, combined with Ca^{2+} channel inhibitor, Ca^{2+} chelator, exogenous Ca^{2+}, and Na-H reverse transporter inhibitor, Na-H exchanger inhibitor, K^+ channel inhibitor, H^+ - ATPase inhibitor,

supplemented by exogenous ROS, to verify whether Ca^{2+} signal is involved in the process of promoting plant Na^+ excretion, vacuolar partition of Na^+ , and K^+ preservation, as well as the Ca^{2+} signal transduction mechanism in this process

II Application cases

1. *Nat Commun*：Ca^{2+}activated 14-3-3 protein acts as a molecular switch in salt stress

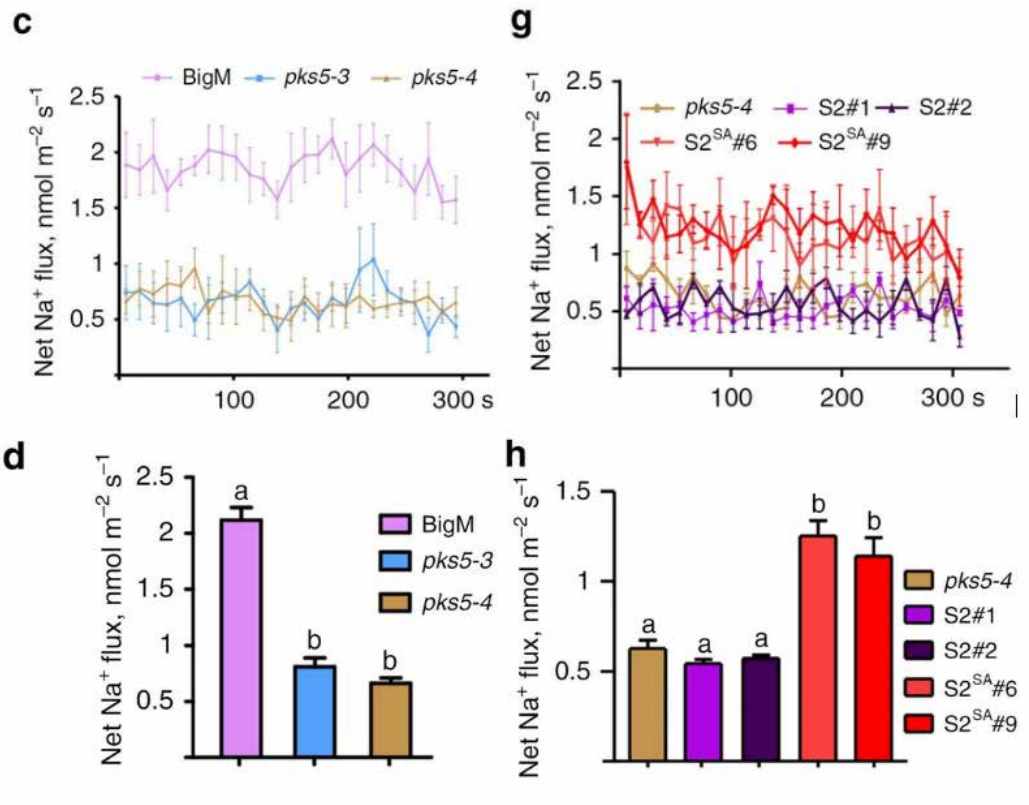

Note. Previous research results show that PKS5 can phosphorylate SOS2 and regulate the activity of SOS2 kinase. Next, we need to determine whether PKS5 affects the salt tolerance of Arabidopsis. Using NMT technology, the Na^+ velocity in the root meristematic zone of 7-day-old seedlings of BigM, *pks5-3* and *pks5-4* was measured after 12 hours of treatment with 100 mM NaCl. The root showed obvious net Na^+ efflux under salt stress, but the efflux rates of *pks5-3* and *pks5-4* were significantly lower than that of BigM (c, d). Overexpression of SOS2 does not improve the salt sensitive phenotype of *pks5-4*. However, the salt sensitive phenotype of *pks5-4* is improved by the expression of $SOS2^{S294A}$. Then this study detected the Na^+ flow rate in the hybrid lines, and found that the expression of $SOS2^{S294A}$ improved the Na^+ flow rate of *pks5-4*, but the expression of SOS2 did not (g, h). Therefore, PKS5 negatively regulates the salt tolerance of Arabidopsis by relying on SOS2Ser294 phosphorylation.

2. *Nat Commun*：Natural variation of calcium-binding protein coding gene endows maize with salt and alkaline tolerance

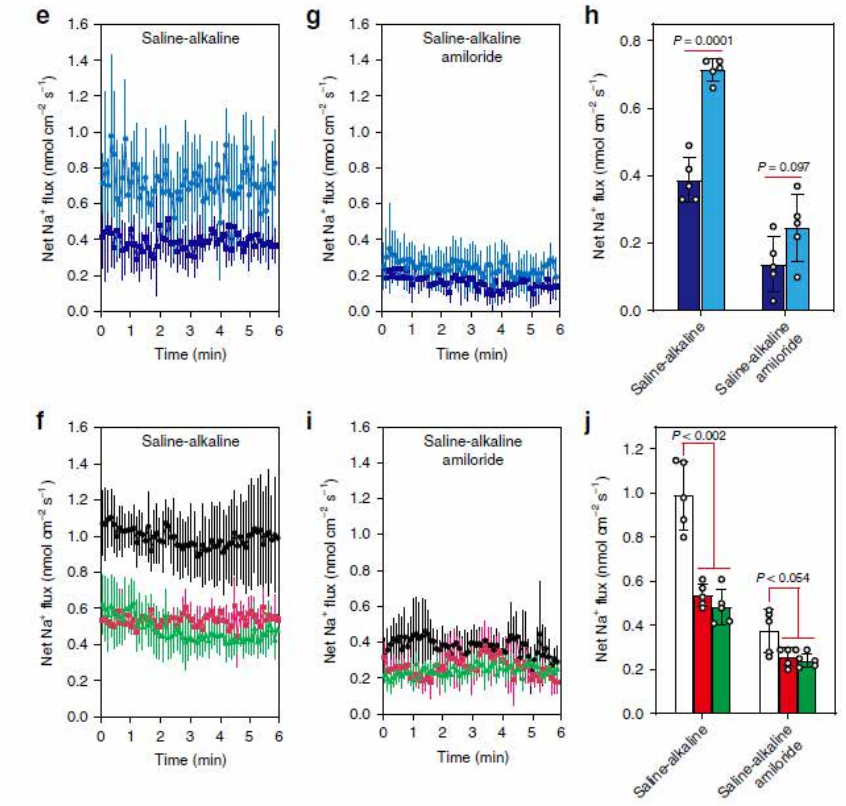

Note: Na^+ flow rate (e-j) in root meristem zone of *ZmNSA1*^{UFMu}, *ZmNSA1* overexpression plants and their wild-type control. The plants aged 5 days were treated with 100mM NaCl (pH 8.0) for 24 hours, and the test solution (e, f) or containing 50 μ M Amilori (g, i) was incubated in the test solution for 30 minutes, and then the Na^+ flow rate was measured using the non-invasive microtest (NMT).

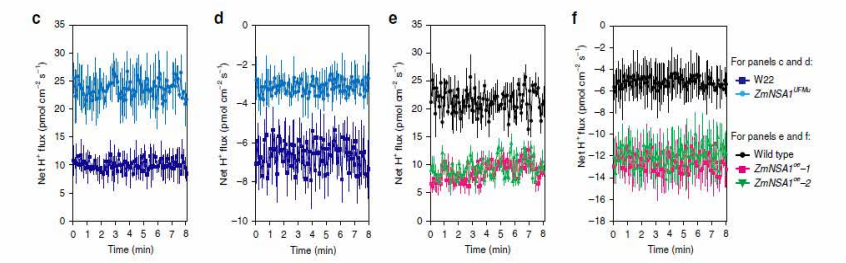

Note. It is found that *ZmNSA1*^{UFMU} has greater H^+ outflow (c, d) than W22, while *ZmNSA1* overexpression plants have lower H^+ outflow (e, f) than wild type plants, which confirms that *ZmNSE1* negatively regulates root H^+ outflow.

Scientific research junction of plant immunity and non-invasive micro-test technology (NMT)

I Summary

1. It is used to quantitatively detect the transmembrane Ca^{2+} absorption in the process of mode immunity (PTI) and effect immunity (ETI), and verify the functions of CNGC, OSCA, NLR, etc

2. Used to quantitatively study the function of Ca^{2+} - ATPase (Ca^{2+} removal rate) and K^+ signal in hypersensitivity reaction

3. It is used to quantitatively study the direction and rate of real-time transmembrane transport of K^+ (GORK: outward K^+ channel) and Cl -/NO3- (SLAC: S-type anion channel) that directly regulate the volume of guard cells in the process of stomatal immunity, and verify the functions of GORK, SLAC, etc

4. It is used to quantitatively study the direction and rate of the transmembrane transport of reactive oxygen species H_2O_2 in the process of plant immunity, and verify the functions of PIP (aquaporin gene)

II Application cases

1. *Cell Res*: Lossless "electrophysiological" calcium flow provides key evidence for CNGC9-mediated PAMP activation of calcium channels to promote rice disease resistance

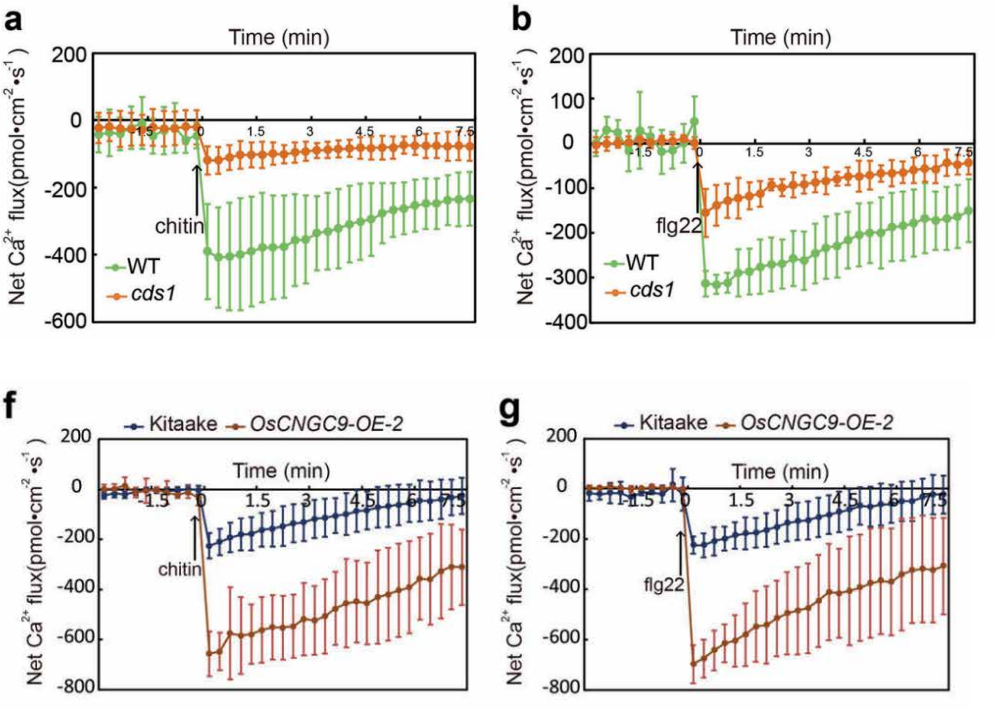

Note. NMT was used to verify the difference of Ca^{2+} uptake (real-time transmembrane Ca^{2+} influx) rate of CNGC9 (membrane calcium channel) and its upstream signal pathway corresponding mutants and overexpressed materials during PTI

2. *Plant Physiol*: NMT found that the interaction of susceptible gene Bln1 and CaM3 induced Ca^{2+} ↓, which provided core evidence for the negative regulation of wheat stripe rust resistance by Bln1

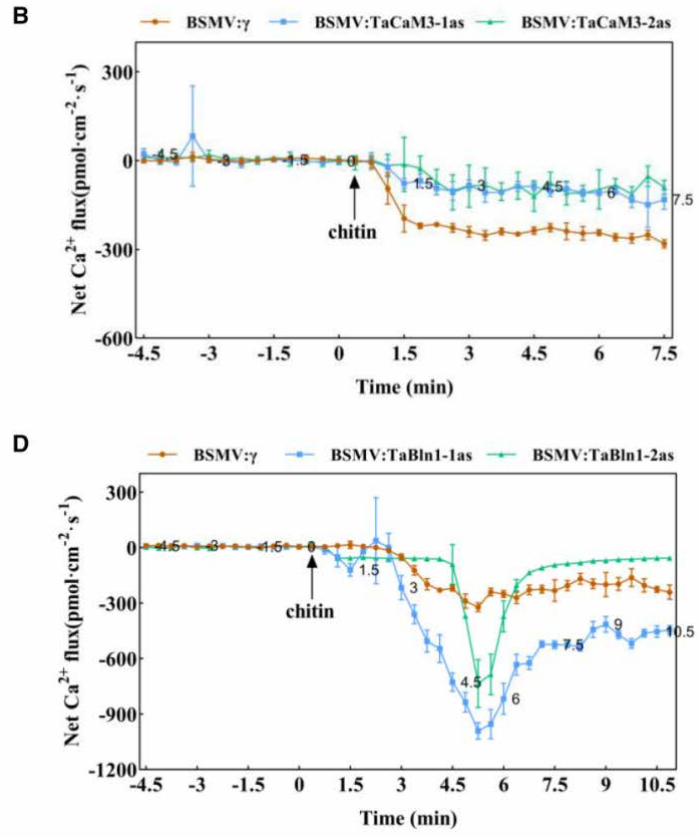

Note: All blades have obvious response to chitin treatment. Under the stimulation of chitin, inoculate BSMV: γ The mesophyll cells of control plants showed strong Ca^{2+} influx; However, TaCaM3 silenced plants had little change. Since TaBln1 can interact with TaCaM3, it is speculated that TaBln1 may also affect Ca^{2+} influx by affecting TaCaM3. To test this hypothesis, the study also detected Ca^{2+} influx in TaBln1 silenced plants. The results showed that compared with the control, the Ca^{2+} influx rate of TaBln1 silenced plants was faster. These results show that TaCaM3 can affect Ca^{2+} influx, which is impaired by the interaction with TaBln1.

3. *Nature*：Non-destructive "electrophysiological" calcium flow provides key evidence for the identification of stomatal immune calcium channel OSCA1.3

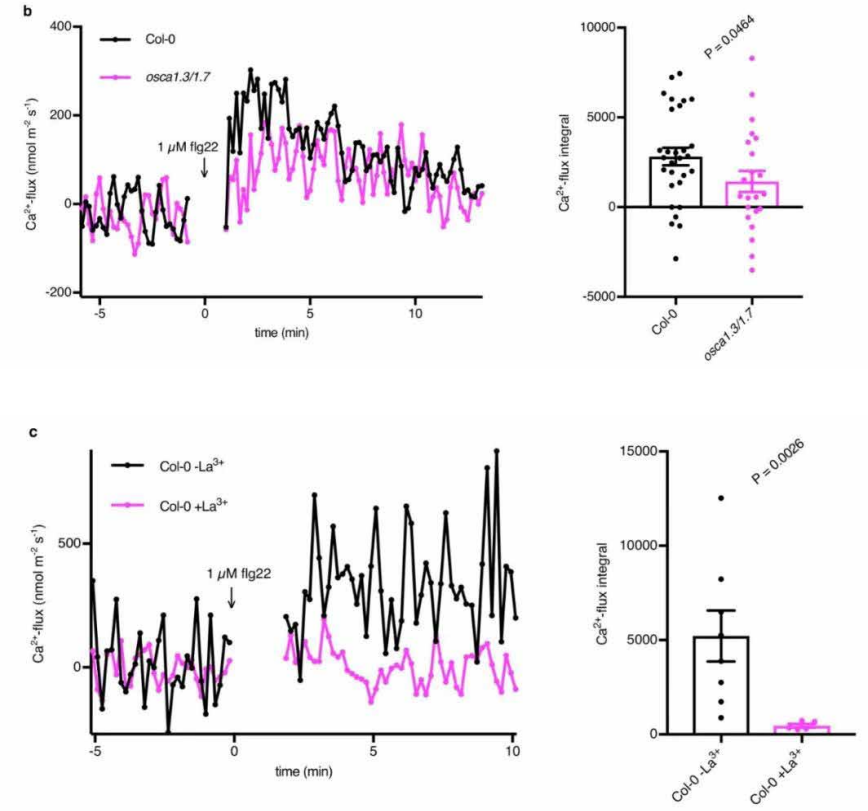

Note. The net Ca^{2+} flow rate of guard cells of Col-0 and *osca1.3/1.7* was measured using non-invasive micro-measurement technology. The results showed that compared with Col-0, the absorption rate of Ca^{2+} in 7 minutes after adding flg22 decreased in *osca1.3/1.7* (b). The Ca^{2+} absorption rate of Col-0 guard cells with or without lanthanum chloride pretreatment was detected. It was found that the Ca^{2+} absorption was significantly blocked within 8 minutes after adding flg22 after lanthanum chloride treatment (c).

4. *Plant Cell Environ*: Mechanism of Ca^{2+} current regulating plant cross tolerance

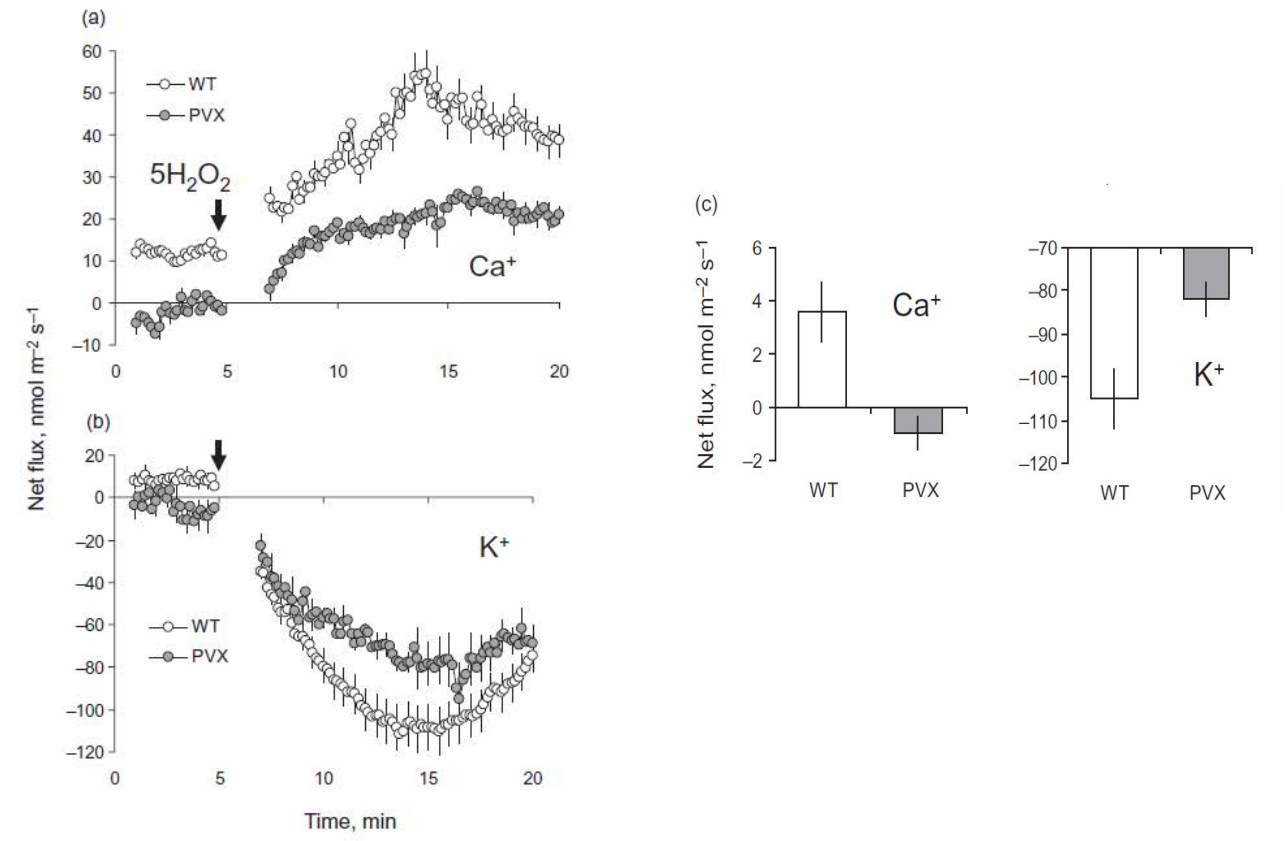

Note: Tobacco was infected with Potato virus X (PVX) and exposed to oxidative stress (UV-C or H_2O_2). The flow rates of Ca^{2+} and K^+ were measured by non-invasive micro-measurement technology. The adaptive response of the whole plant was studied by combining pharmacological and cytological methods. It was found that the plant could better cope with UV and H_2O_2 after being infected by the virus and prevent the damage of chloroplast structure and function. Ca^{2+} flow is the early response of plants to pathogen invasion. Ca^{2+} transmission and ROS may be the key to control the cell-level cross tolerance.

Scientific research combination of temperature stress and non-invasive micro-test technology (NMT)

I Summary

Taking the quantitative detection of real-time Ca^{2+} uptake rate of root, mesophyll and other materials under temperature stress as the foothold, verify the Ca^{2+} signal related pathways such as Cold1, CNGC9, HST1, SCT1, etc

II Application cases

1. *Cell*: Lossless "electrophysiological" calcium flow provides direct evidence for revealing the molecular mechanism of rice's perception of cold damage

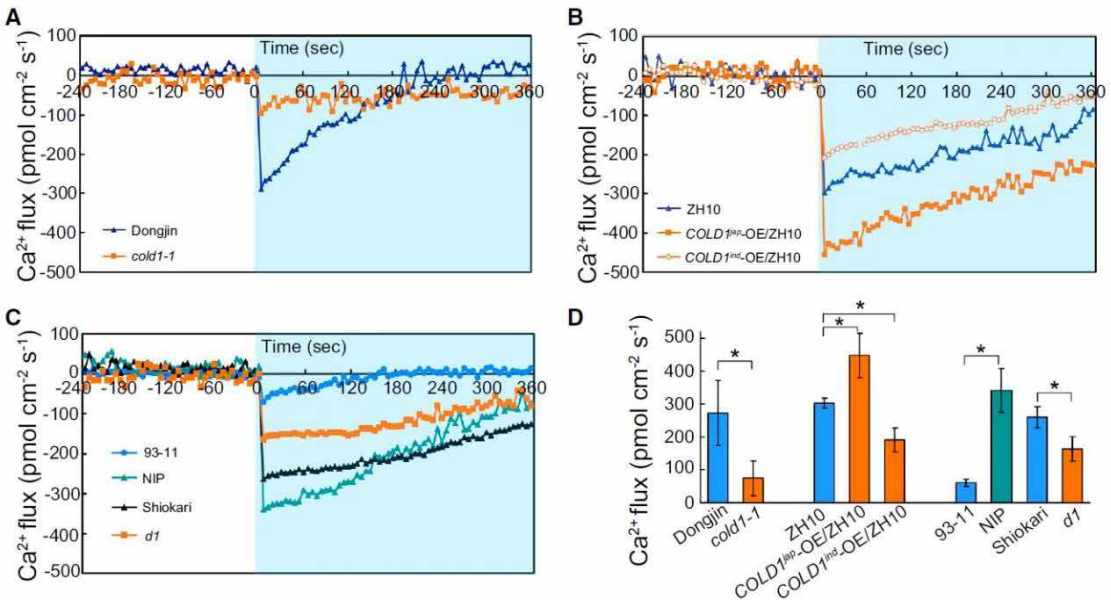

Note: The flow rate of Ca^{2+} in rice roots under cold shock was studied by NMT. Under the stimulation of low temperature, there was a large amount of extracellular Ca^{2+} influx in the root of wild type Dongjin rice, and there was a negative peak (A). In contrast, under the same conditions, the NMT signal of cold1-1 has no obvious change. Compared with the wild-type ZH10 rice, the COLD1jam transgenic line had more significant Ca^{2+} influx under low temperature treatment, but the COLD1ind transgenic line was less obvious (B). Compared with indica 93-11, Nipponbare's reaction was stronger (C). In addition, the Ca^{2+} influx rate of RGA1 mutant d1 was lower than that of wild type Shiokari. The average maximum inflow rate after cold shock between cold 1-1 or transgenic lines and wild type was significantly different (D).

2. *Nat Plants*: "Non-destructive electrophysiology" transmembrane Ca^{2+} flow provides evidence for G protein to regulate wax synthesis through calcium signal and thus regulate rice heat tolerance

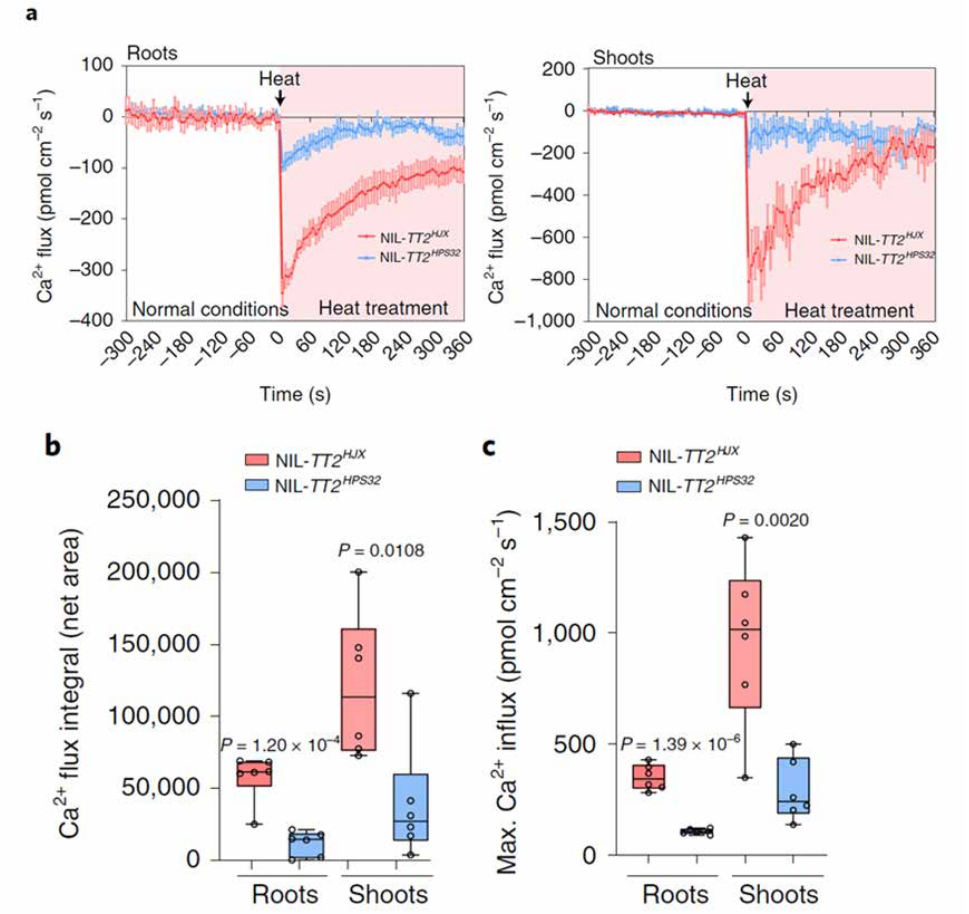

Note: The research uses the non-destructive micro-measurement technology (NMT) to detect the root and aboveground parts of rice under thermal stimulation. Under normal conditions, the NMT signals in the root and aboveground parts of the two NILs have no difference (a). Under thermal stimulation, significant Ca^{2+} influx was detected in the root and aboveground parts of NIL-$TT2^{HJX}$ (a). In contrast, the change of Ca^{2+} flow rate signal of NIL-$TT2^{HPS32}$ is not obvious under the same thermal stimulation (a). Under thermal stimulation, the average Ca^{2+} flow rate integral and the average maximum Ca^{2+} flow rate of NIL-$TT2^{HJX}$ were significantly higher than those of NIL-$TT2^{HPS32}$ (b, c). The fluctuation of extracellular Ca^{2+} influx caused by thermal stimulation indicates that the increase of cytoplasmic Ca^{2+} concentration caused by extracellular Ca^{2+} may be significantly inhibited due to the loss of *TT2* function.

Water and drought stress and non-invasive micro-test technology (NMT) scientific research junction

I Summary

1. Quantitative detection of root H^+ - ATPase inhibition system (H^+ transport rate) under drought stress provides evidence for revealing drought tolerance mechanism

2. Quantitative detection of the ability of plant root and mesophyll to regulate K^+ homeostasis under drought stress

3. Quantitative detection of transmembrane Ca^{2+} flow under drought stress reveals the mechanism of Ca^{2+} signal participating in ABA and other signal transduction pathways

4. Quantitative detection of transmembrane Ca^{2+} flow under flooding stress reveals the mechanism of CBL and other regulatory Ca^{2+} signals

5. Quantitative detection of ROS (H_2O_2) transmembrane transport rate under drought stress

II Application cases

1. *Plant Biotechnol J* HvAKT2 and HvHAK1 improve drought tolerance by enhancing the mesophyll H^+ homeostasis

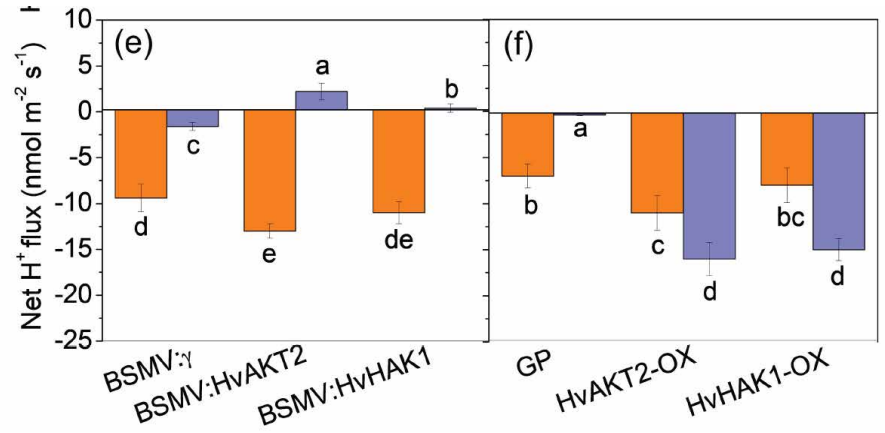

Note: Drought (20% PEG treatment for 1 h) led to the transformation of leaf mesophyll H^+ from efflux to inward flow in drought-sensitive barley inoculated with BSMV: HvAKT2 and BSMV: HvHAK1 (e). On the contrary, compared with Golden Promise, overexpression of *HvAKT2* and *HvHAK1* significantly increased mesophyll response to drought stress (f).

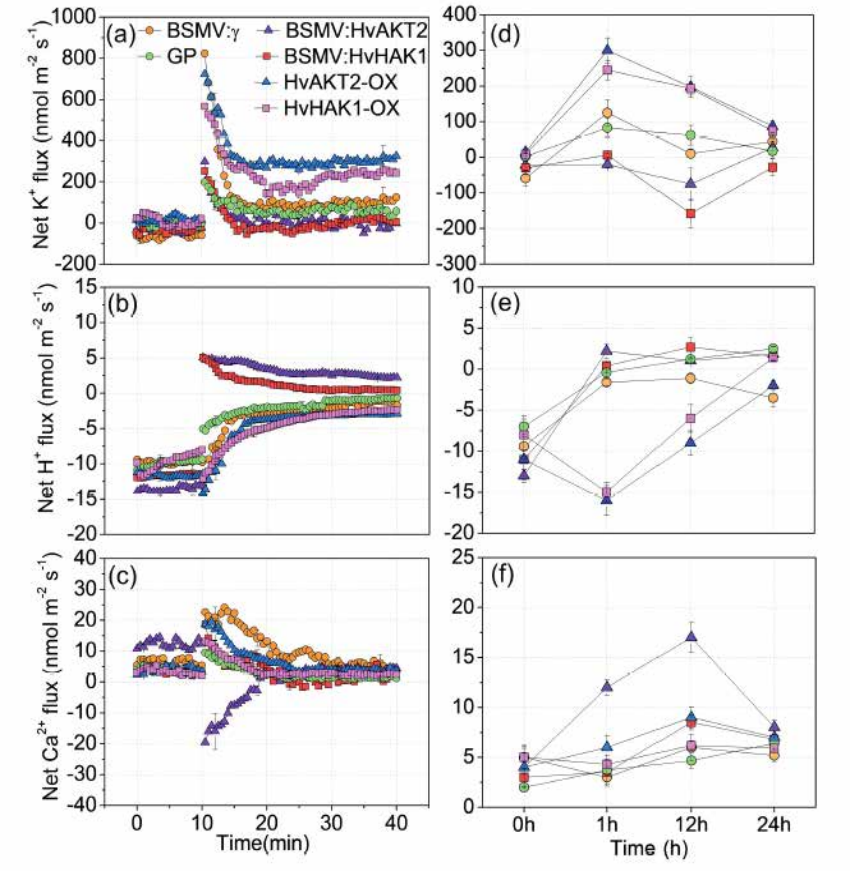

Note. Then the K^+, H^+ and Ca^{2+} flow rates of all barley lines (XZ5, silent lines, Golden Promise and overexpression lines) were measured within 24 hours to understand the role of *HvAKT2* and *HvHAK1* in barley drought resistance. Compared with the control, K^+ uptake in mesophyll tissue of silent *HvAKT2* and *HvHAK1* lines was significantly reduced (a, d) after PEG-induced drought stress for 1 and 12 hours. The simulated inoculated plants showed H^+ efflux in the leaves of the control group and the plants treated with PEG-induced drought, while the plants silenced by *HvAKT2* - and *HvHAK1* - showed H^+ influx (b, e) after PEG-induced drought. BSMV: The flow rate of Ca^{2+} in mesophyll cells of HvHAK1 plant leaves increased significantly after 1 h and 12 h of drought treatment (c, f). Similar K^+, H^+ and Ca^{2+} flow rates were observed at the root of the silent strain.

In the mesophyll tissue of plants overexpressing *HvAKT2* and *HvHAK1*, PEG-induced drought stress resulted in the K^+ influx rate of HvAKT2-OX and HvHAK1-OX plants 2.6 and 1.8 times higher than that of Golden Promise (a). In all plants, after PEG treatment for 24 hours, the K^+ influx rate decreased, but in the overexpression strains, the K^+ influx rate (70-80 nmol $m^{-2}s^{-1}$) was still significantly higher than the control (a, d). After 1 h and 12 h of control and PEG-induced drought treatment, plants overexpressing HvAKT2 and HvHAK1 maintained more significant H^+ efflux (b, e) than Golden Promise. The flow rate of Ca^{2+} in mesophyll cells of leaves of HvAKT2-OX plant increased significantly after 1 h and 12 h of drought (c, f).

2. *Front Plant Sci*: Ca^{2+}uptake by roots is critical to root elongation under water stress

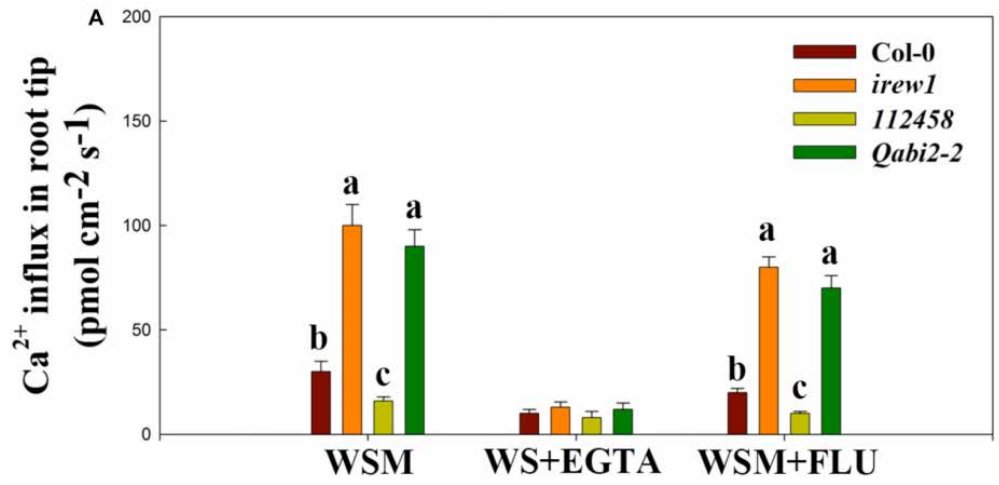

Note. Under WSM conditions, the Ca^{2+} internal flow of irew1 and *Qabi2-2* is significantly higher than that of *Col-0* and *112458*. Although the Ca^{2+} influx decreased sharply under the treatment of WSM+10 mM EGTA, the Ca^{2+} influx decreased less under the treatment of WSM+10 mM FLU, indicating that ABA had little effect on the Ca^{2+} influx under WSM.

Scientific research joint of reproductive growth and development and non-invasive micro-test technology

I Summary

1. Quantitative detection of real-time Ca^{2+} and H+signals in different parts of the pollen tube, cotton fiber and root hair during the polar growth process, characterizing the dynamic steady state of Ca2+ concentration gradient and pH gradient of polar growth cells;

2. Dynamic pH and transmembrane Ca^{2+} flow detection during pollen and stigma recognition;

II Application cases

1. *Science*：NMT found that the intracellular transport of glutamate receptor-like channels affected the calcium flow in pollen tubes

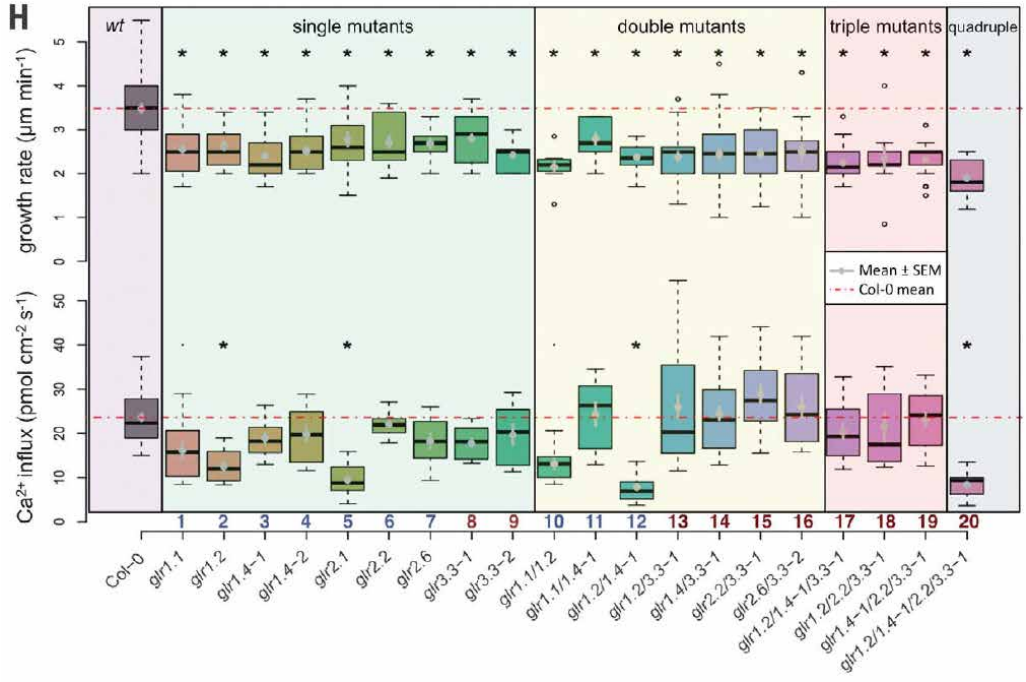

Note: The arrangement and activation of glutamate receptor channels (GLRs) are related to CNIH protein. The result in the lower part of the figure above is the rate of Ca^{2+} uptake by the pollen tube of the single mutant Arabidopsis GLRs (AtGLRs) expressed in the pollen tube; However, the higher-order mutant AtGLR3.3 showed the opposite phenomenon. These differences can be explained by subcellular AtGLR localization. Researchers also discussed the significance of AtCNIHs in such sequencing. They found that the interaction between AtGLRs and AtCNIH pairs produced specific intracellular localization points. In mammalian cells without ligands, AtCNIHs further triggered AtGLR activity. These data and results jointly reveal a mechanism that AtCNIHs cause changes in the distribution and activity of AtGLRs, thus regulating Ca^{2+} homeostasis.

2. *Nature Commun*：NMT provides direct evidence for proton pump to stimulate pollen tube growth and support cell polarity

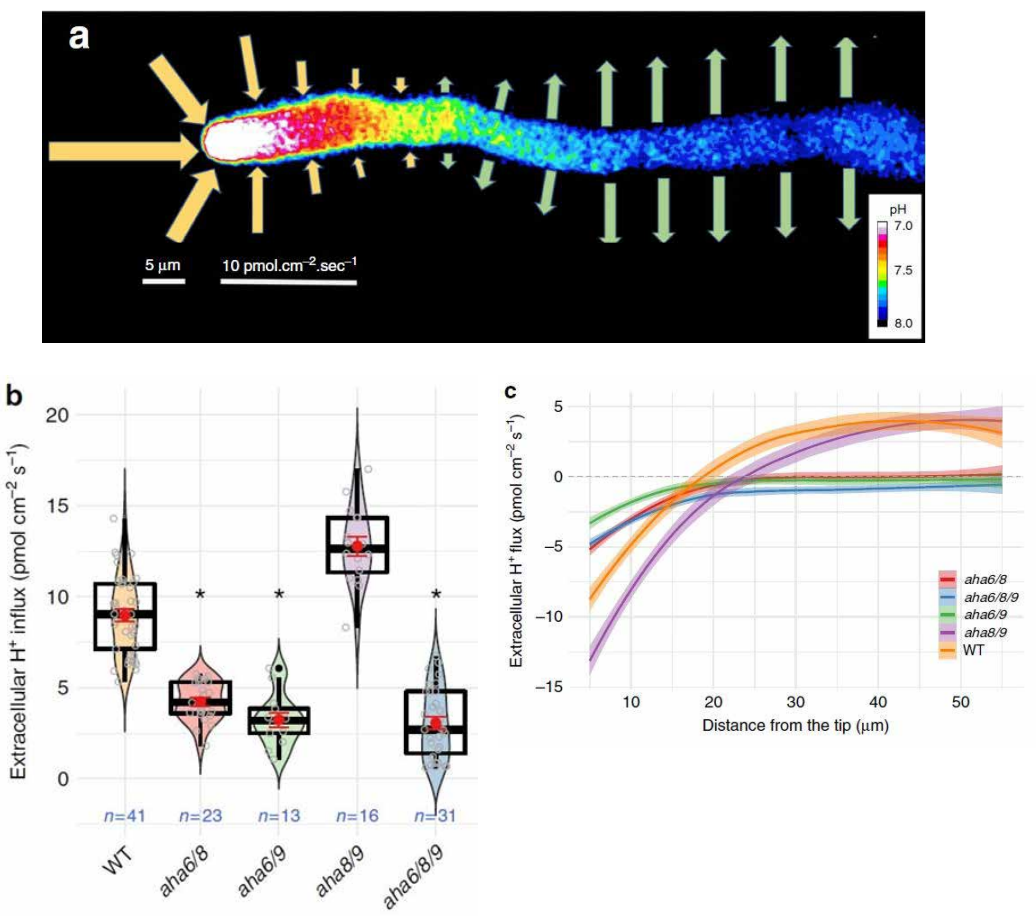

Note. The pollen tube was measured by NMT and its transmembrane H^+ flow was detected. The H^+ flow results could characterize the activity of AHA. The growth rate of all mutant combinations lacking AHA6 decreased, which was related to the reduction of H^+ absorption at the tip (b), the reduction of stem efflux and the retraction of the boundary point of absorption/efflux to the stem (c), especially in the triple mutant. The wild-type pollen tube showed that the absorption of H^+ at the top reversed to the outer row (c) at about 15-20 um from the top, while almost all the mutant combinations lacking AHA6 did not follow the H^+ outer row of the pollen tube. Although aha8/9 shows a reversal point (c) more than 20 um from the tip, the absorption of the tip and the outer row along the handle are similar to those of the wild type.

3. *Plant Cell*：NMT provides a basis for a new regulatory mechanism of root hair development

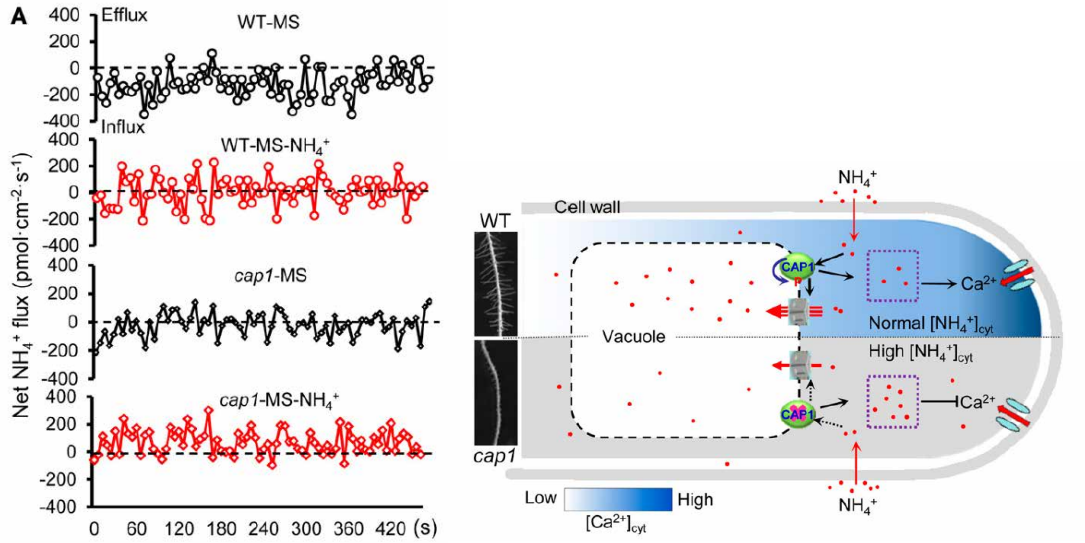

Note. The flow rate of Ca^{2+} at the tip of root hairs and NH_4^+ in vacuoles was measured by using the non-damage micro-measurement technology (NMT). It was found that the concentration of Ca^{2+} at the tip of root hairs was in a steady state of gradient distribution during normal growth and development, which was regulated by intracellular NH_4^+. When the concentration of NH_4^+ in the environment is too high, the normal distribution of Ca^{2+} concentration gradient will be destroyed. In order to maintain the normal growth of root hairs, when the concentration of NH_4^+ increases, the intracellular calcium associated protein kinase (CAP) located in the vacuole membrane will partition the excess NH_4^+ into the vacuole to maintain the Ca^{2+} concentration gradient required for the normal growth of root hairs. When CAP1 is knocked out, the root hairs cannot grow in normal medium (MS), and if the concentration of NH_4^+ (MS-NH_4^+) is reduced in the growth environment, the root hairs return to the normal polar growth state.

Combination of plant hormones and non-invasive micro-test technology (NMT)

I Summary

1. Quantitative detection of transmembrane IAA transport rate in living plants

2. Study the mechanism of ABA, JA, melatonin, gibberellin and other regulating plant physiological processes

II Application cases

1. *Plant Commun*：NMT monitoring of IAA flow in living roots confirmed that OsHAK5 regulates auxin transport and regulates rice plant type

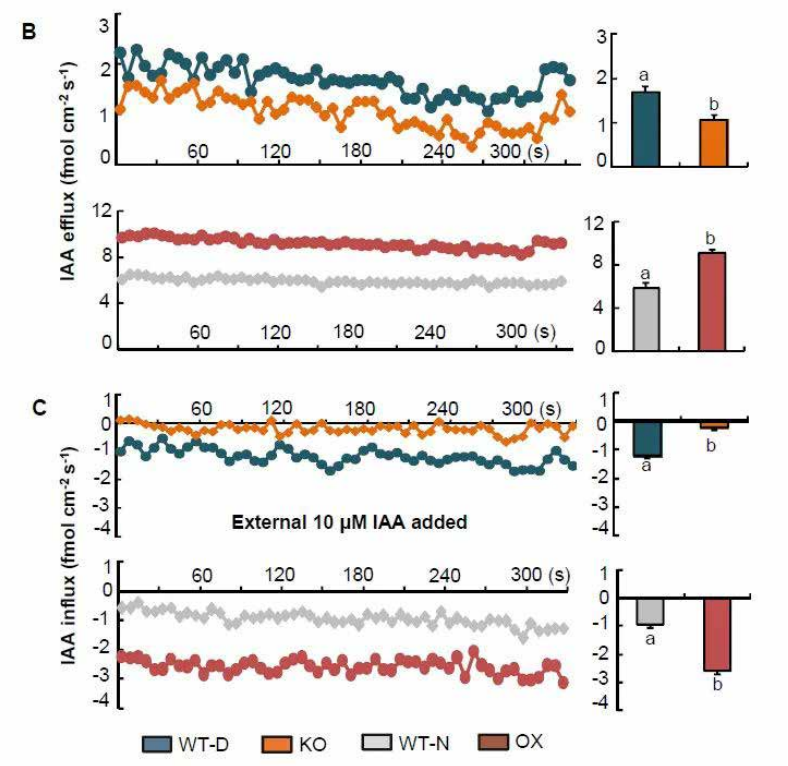

Note: The process of IAA outflow (B) and inflow (C) in the primary root meristem of seedlings was monitored by NMT. At 10 μM Measure the inflow of IAA in the presence of external IAA. The histogram shows the average outflow rate and net inflow rate in the whole 5 minutes. Among them, OsHAK5 KO inflow is relatively small, and OsHAK6 OX inflow has increased.

2. *Nature*：Non-damage micro-measurement technology found that IAA could promote root uptake of H^+ and alkalization of exoplasts, providing important evidence for the mechanism of auxin "acid growth hypothesis"

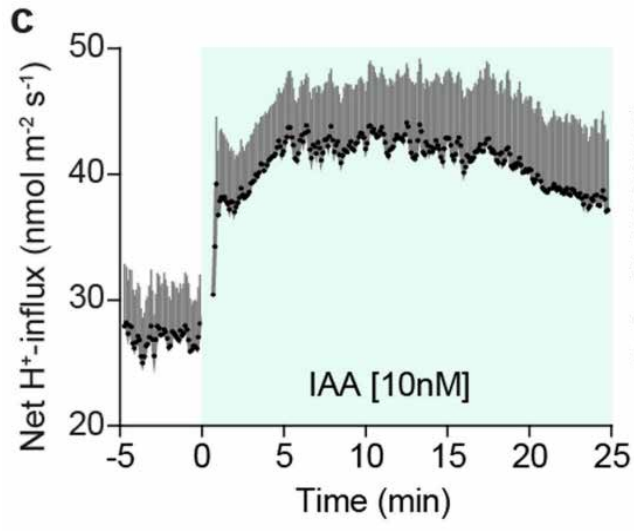

Note to the figure. Using PM-Cyto reporter to monitor the intracellular pH value, it was found that after 5 nM IAA treatment, the pH value of adjacent cytoplasm of plasma membrane (PM) decreased at the same time. The simultaneous increase of extracellular pH and the decrease of intracellular pH mean that H+flows into cells. The H+flow rate of root epidermal cells in the elongation zone after IAA treatment was monitored by non-invasive micro-measurement technology, and the H+influx was indeed found, which was consistent with the similar observation results in root hair cells. Auxin causes rapid alkalization of extracellular bodies by increasing the inflow of intracellular H+. The spatiotemporal correlation between this process and root growth inhibition showed that the extracellular alkalization was a potential cellular mechanism for root growth inhibition.

3. *Plant Cell*: NMT found that ABA promoted the secretion of H^+(cytoplasmic alkalization) from guard cells dependent on BAK1 and AHA2, providing evidence for AHA2 to participate in ABA-induced stomatal closure under drought

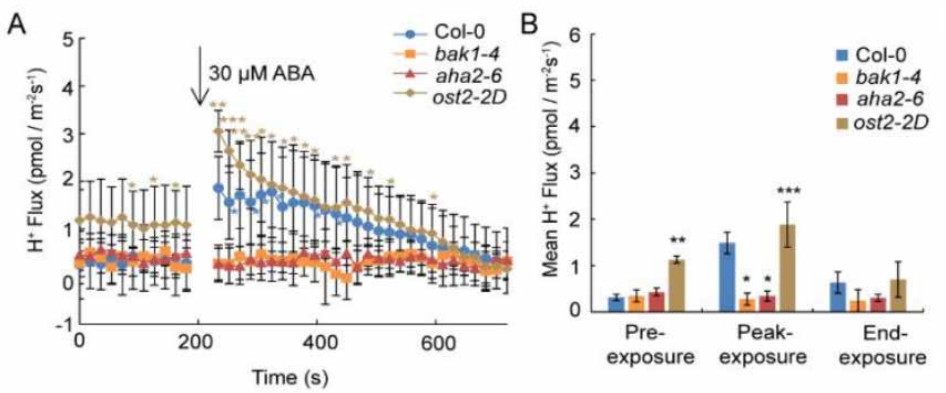

Note. In order to study the role of AHA2 and its activation by BAK1 in ABA-induced transmembrane ion efflux of guard cells, the research used the non-invasive micro-measurement technique (NMT) to detect the H^+ transport in the guard cells of Col-0, *AHA2-6*, *BAK1-4* and *ost2-2D* plants. Instantaneous addition 30 μ M ABA can cause Col-0 and $^{ost2\text{-}2D}$ guard cells to show obvious H^+ transmembrane efflux, and *ost2-2D* is stronger than Col-0 H^+ efflux. After exogenous ABA treatment, H^+ efflux quickly recovered from peak to near baseline level. In addition, a large number of H^+ in Col-0 and *ost2-2D* guard cells were pumped out to the extracellular body. In contrast, the transmembrane H^+ flow of aha2-6 and bak1-4 guard cells did not respond to exogenous ABA. These results showed that ABA could rapidly induce the instantaneous outflow of H^+ in guard cells, which depended on BAK1 and AHA2.

The scientific research point of plant-microorganism interaction and non-invasive micro-test technology (NMT)

I Summary

1. Quantitative study of dynamic pH (H^+ transmembrane transport) and ROS signal between "root and mycelium"

2. Quantitative detection of the effect of nodule remediation on degradation of organic pollutants

3. Remediation of heavy metal pollution, see chapter "heavy metal" for details

4. See the section "Reproductive growth and development" for the role of promoting growth

5. Plant-pathogen interaction

6. For other cross studies, see nutrient elements, drought, heavy metals, etc

II Application cases

1. *Plant Cell Environ*: Root endophytic fungi regulate the nitrogen flux at the interaction interface and affect the host response to different nitrogen forms

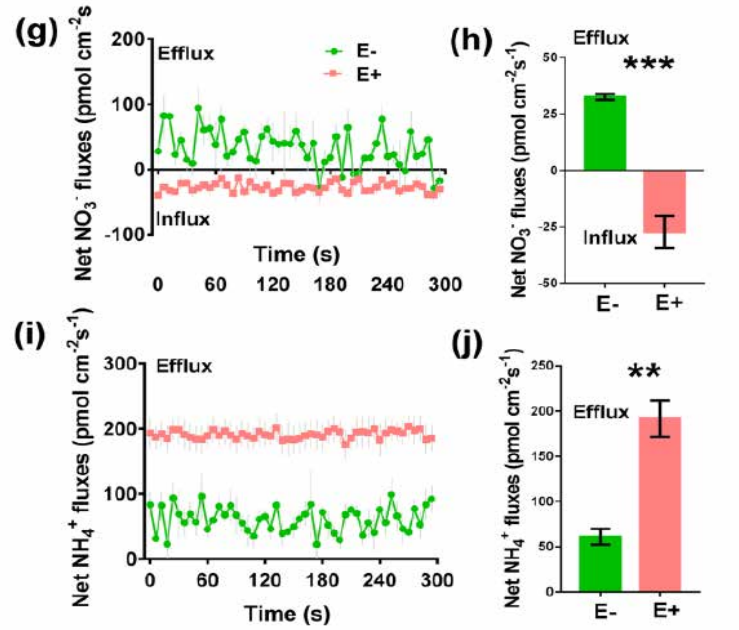

Note. The paper studies the dynamics of net inorganic nitrogen around the root tip under NO_3^- or NH_4^+ nutrition, because the regulated ion flux on the root plasma membrane is related to plant growth and ion accumulation. Compared with uninoculated mycorrhizal fungi, the root tip colonized by fungi showed significant NO_3 inflow (g, h). In addition, uninoculated mycorrhiza showed moderate NH_4^+ outflow (i, j), which was consistent with the previously observed symptoms of elevated NH_4^+ level, while fungal colonization roots showed about 3.13 times high NH_4^+ outflow. It is noteworthy that the increase of NH_4^+ efflux induced by fungi is positively correlated with the decrease of plant growth.

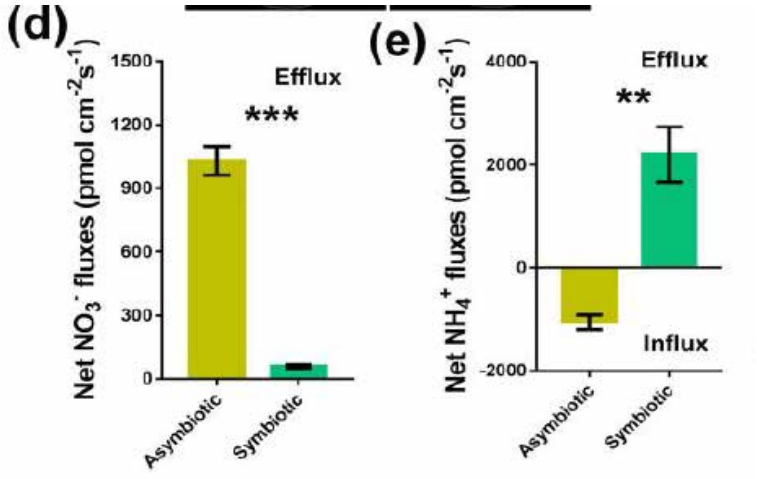

Note. The NO_3 emission at the top of symbiotic mycelium is lower than that of non-symbiotic mycelium, which may retain NO_3 nutrition for mycelium growth (d). The top of symbiotic hypha showed obvious NH_4^+ outflow, while the top of non-symbiotic hypha showed NH_4^+ inflow (e). These results showed that during the interaction with Arabidopsis, Pteropus stenoptera maintained NO3 -, but excluded NH_4^+.

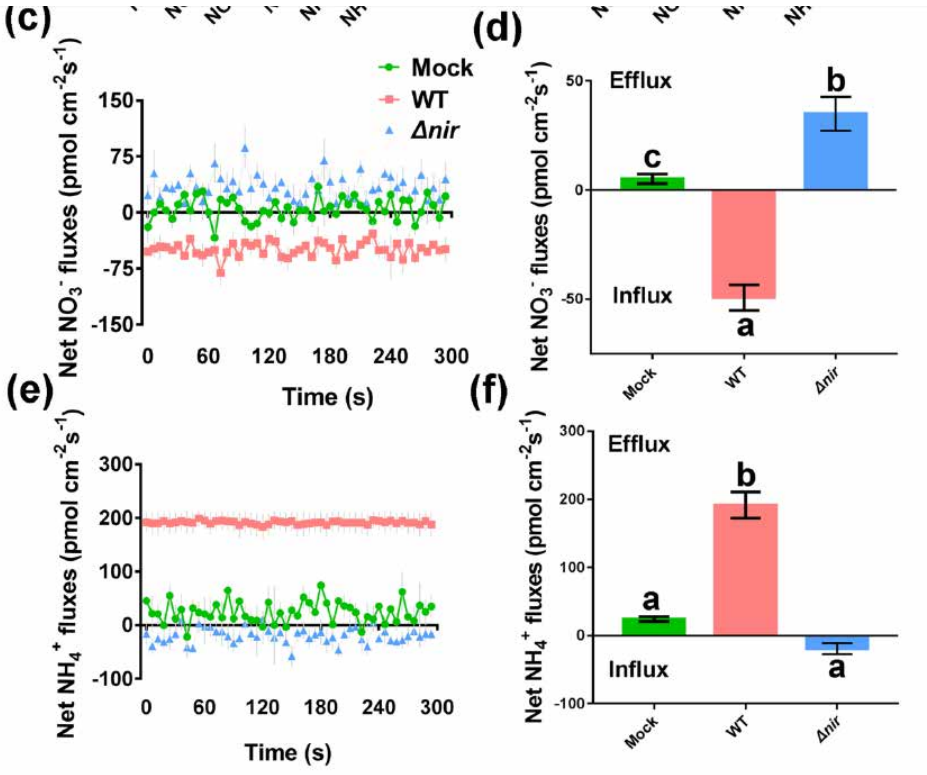

Note. Compared with wild type inoculated roots, Δ The roots inoculated with nir showed an increase in NO_3 outflow under NO_3 nutrition (c d) and an obvious inflow of NH_4^+ under NH_4^+ nutrition (e f). Compared with the non-inoculated samples under NH_4^+ nutrition, Δ The root colonization of nir strain damaged the increase of NO_3^- content in buds induced by WT under NO_3^- nutrition, and led to the decrease of NH_4^+ content in seedlings.

2. *Environ Sci Technol*: NMTvalidation of nodule promoting degradation of polychlorinated biphenyls

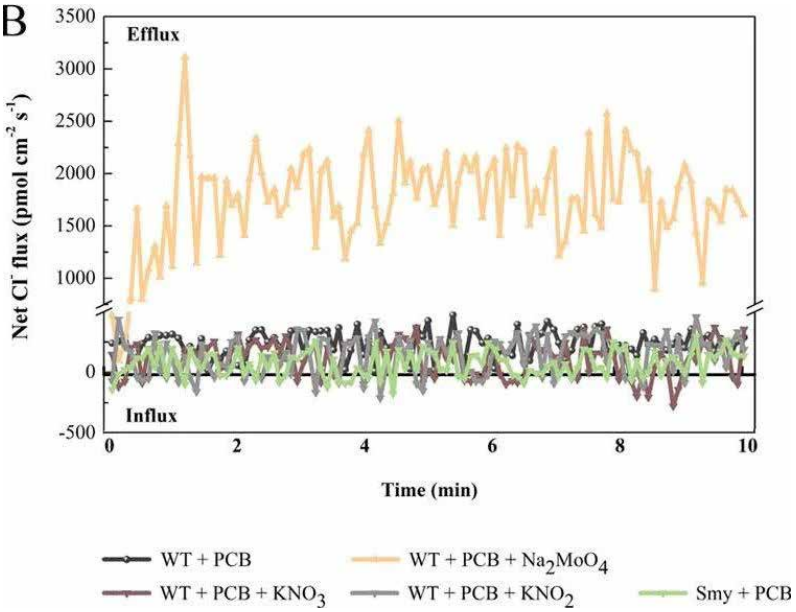

Note. By quantifying the net flow rate of Cl^-, the dechlorination activity (B) of microaerobic nodules supplemented by PCB 77 was determined. The addition of PCB led to a significant increase in the rate of Cl^- efflux in the nodule inoculated with strain WT (P<0.05), indicating that the compound was dechlorinated in the micro-oxybacteria. Consistent with the N_2 fixation activity, the Cl^-efflux rate increased by 7.2 times after MoO_4^{2-} treatment compared with the control (P<0.05). In contrast, after adding NO_3^-, the average efflux rate of Cl - decreased by 29% compared with the control (WT+PCB) (P<0.05), while after NO_2^- treatment, the average efflux rate of Cl^- only changed slightly (P>0.05). In the plants lacking the nifA mutant lacking nitrogenase activity, the rate of Cl^-efflux was 72% lower than that of WT treatment (P<0.05). However, in the mutation group, the Cl^-efflux did not increase significantly after PCB treatment (P>0.05), indicating that the dechlorination effect may be very weak under these conditions.

3. *Curr Biol*：NMT provides a basis for revealing the regulatory effect of magnesium on carbon and nitrogen nutrient exchange in soybean nodules

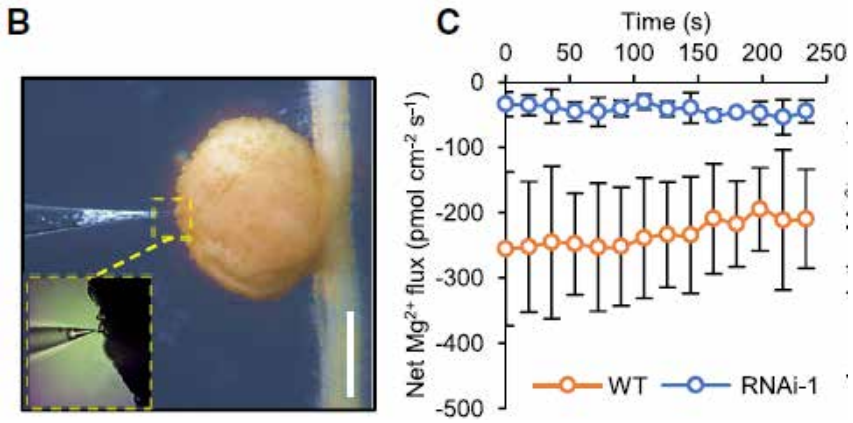

Note. The use of NMT to monitor the net flow rate of magnesium in real time (B) shows that by knocking out the expression of GmMGT4 and 5, the input amount of magnesium in nodules is significantly reduced (C), which leads to a significant reduction in the cumulative amount of magnesium in nodules. It provides a basis for the regulation of carbon - nitrogen nutrient exchange in soybean nodules.

Scientific research junction of calcium signal and non-invasive micro-test technology (NMT)

I Summary

1. Quantitatively detect the real-time transmembrane Ca^{2+} flow of living cells and tissues, and verify the functions of CNGC, GLR, OSCA, NLR, TPC, etc

II Application cases

1. *Science*：NMT found that the intracellular transport of glutamate receptor-like channels affected the calcium flow in pollen tubes

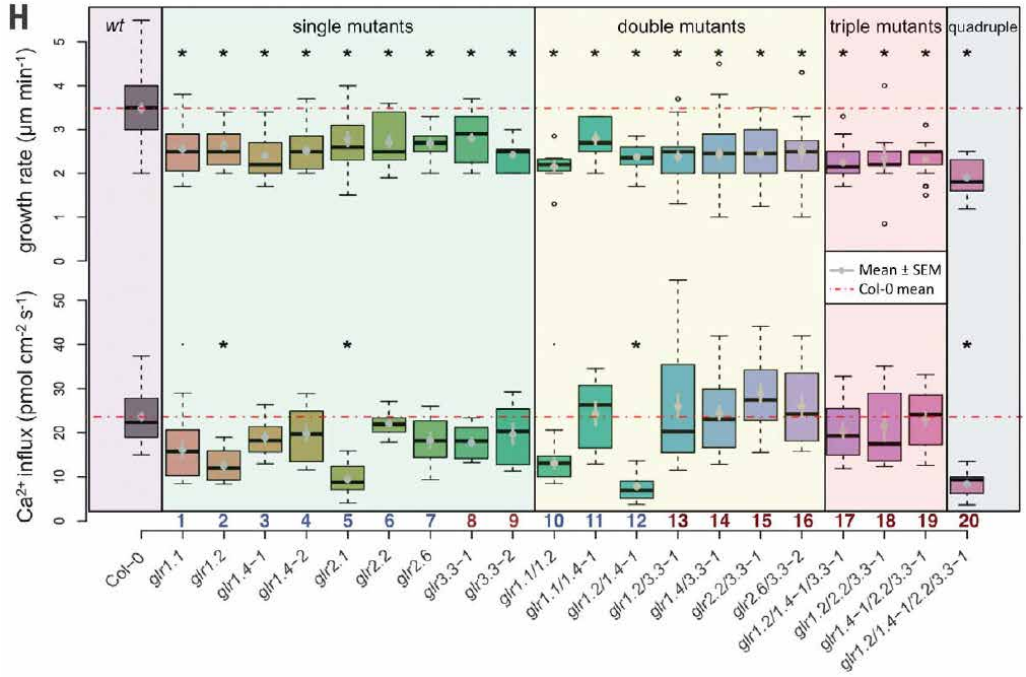

Note: The arrangement and activation of glutamate receptor channels (GLRs) are related to CNIH protein. The result in the lower part of the figure above is the rate of Ca^{2+} uptake by the pollen tube of the single mutant Arabidopsis GLRs (AtGLRs) expressed in the pollen tube; However, the higher-order mutant AtGLR3.3 showed the opposite phenomenon. These differences can be explained by subcellular AtGLR localization. Researchers also discussed the significance of AtCNIHs in such sequencing. They found that the interaction between AtGLRs and AtCNIH pairs produced specific intracellular localization points. In mammalian cells without ligands, AtCNIHs further triggered AtGLR activity. These data and results jointly reveal a mechanism that AtCNIHs cause changes in the distribution and activity of AtGLRs, thus regulating Ca^{2+} homeostasis.

2. *Nature*：Non-destructive "electrophysiological" calcium flow provides key evidence for the identification of stomatal immune calcium channel OSCA1.3

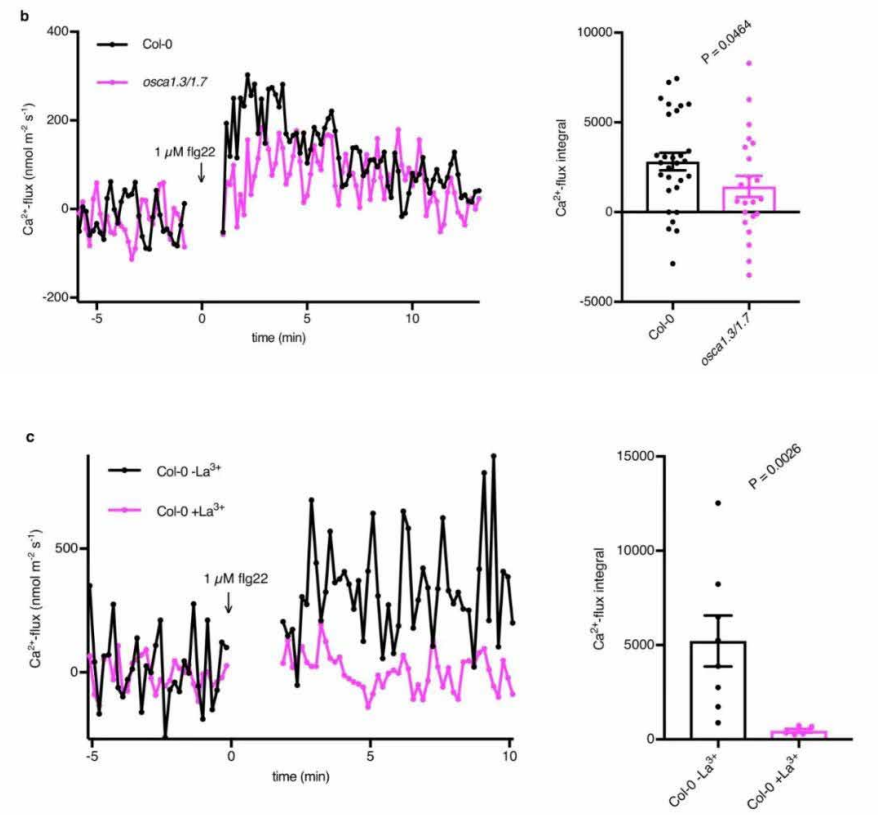

Note. The net Ca^{2+} flow rate of guard cells of Col-0 and *osca1.3/1.7* was measured using non-invasive micro-measurement technology. The results showed that compared with Col-0, the absorption rate of Ca^{2+} i n 7 minutes after adding flg22 decreased in *osca1.3/1.7* (Fig. b). The $CaCa^{2+}$ a bsorption rate of Col-0 guard cells with or without lanthanum chloride pretreatment was detected, and it was found that after lanthanum chloride treatment, the Ca^{2+} absorption was significantly blocked within 8 minutes after adding flg22 (Fig. c).

3. *Cell Res*： Non-destructive "electrophysiological" calcium flow provides key evidence for CNGC9-mediated PAMP-activated calcium channel to promote rice disease resistance

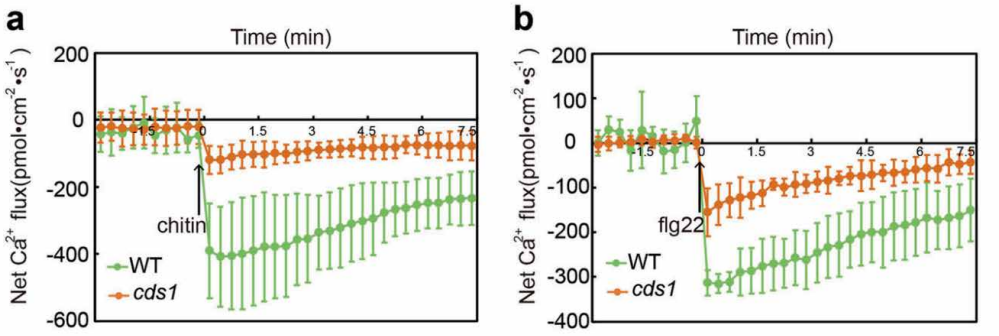

Note. The research uses NMT technology to study whether *OsCNGC9* can mediate Ca^{2+} influx in PTI by measuring the dynamic changes of Ca^{2+} flow rate in mesophyll cells after treatment with two kinds of PAMPs (chitin or flg22). Previous studies have shown that these PAMP elicitors can trigger PTI signals in plants. Under the stimulation of chitin or flg22, WT mesophyll cells showed strong and rapid Ca^{2+} influx (a, b). These results showed that *OsCNGC9* could mediate Ca^{2+} influx in rice PTI, while the ability of cds1 mutant was impaired.

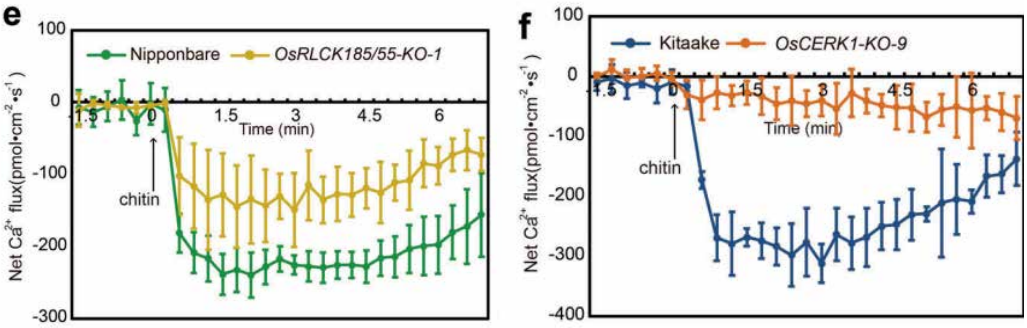

Note. Ca^{2+} flow rate analysis showed that under the stimulation of chitin, Nipponbare mesophyll cells showed rapid Ca^{2+} influx (e). In addition, no obvious Ca^{2+} influx (f) was observed after chitin treatment of Oscerk1 gene knockout mutant.

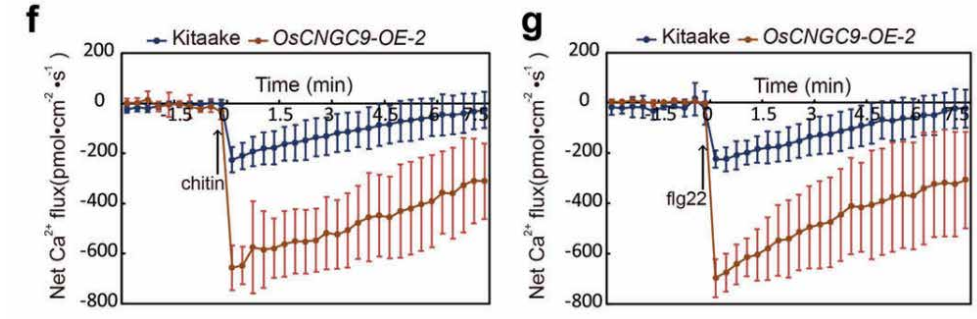

Note: Compared with Kitaake plant, mesophyll cells of *OsCNGC9-OE* transgenic plant showed stronger Ca^{2+} influx (f, g) after stimulation by PAMPs.

Scientific research combination of proton pump and non-invasive micro-test technology (NMT)

I Summary

1. Quantitative detection of real-time transmembrane H^+ flow of living cells and tissues, verification of AHA, OSA, PMA, VHA and other functions

II Application cases

1. *Nature*: Non-invasive micro-test technology found that IAA could promote root uptake of H^+ and alkalization of exoplasts, providing important evidence for the mechanism of auxin "acid growth hypothesis"

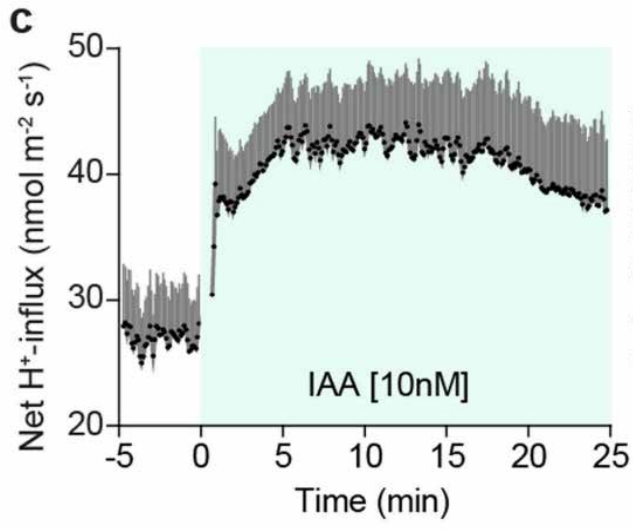

Note. Using *PM-Cyto* reporter to monitor the intracellular pH value, it was found that after 5 nM IAA treatment, the pH value of adjacent cytoplasm of plasma membrane (PM) decreased at the same time. The simultaneous increase of extracellular pH and the decrease of intracellular pH mean that H^+ flows into cells. The H^+ flow rate of root epidermal cells in the elongation zone after IAA treatment was monitored by non-invasive micro-measurement technology, and the H^+ influx was indeed found, which was consistent with the similar observation results in root hair cells. Auxin causes rapid alkalization of extracellular bodies by increasing the inflow of intracellular H^+. The spatiotemporal correlation between this process and root growth inhibition showed that the extracellular alkalization was a potential cellular mechanism for root growth inhibition.

2. *Nat Commun*：NMT found that proton pump gene OAS1 promoted rice root H+ excretion and improved nitrogen absorption

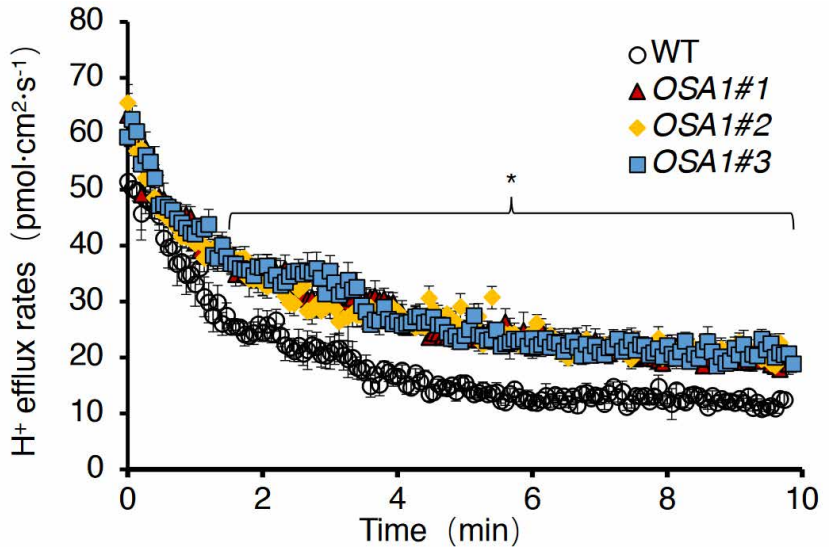

Note. The study used the non-destructive micro-measurement technology (NMT) to detect the change of H^+ transmembrane transport rate in rice roots. The results showed that after 12 hours of treatment with 2 mM NH_4^+ , the H^+ efflux rate of the three OSA1 overexpression lines increased, and was significantly stronger than WT, indicating that the OSA1 overexpression lines promoted NH_4^+ absorption by pumping out more H^+, effectively reducing the concentration of H^+ in the roots, and promoting NH_4^+ assimilation.

3. *Nature Commun*：NMT provides direct evidence for proton pump to stimulate pollen tube growth and support cell polarity

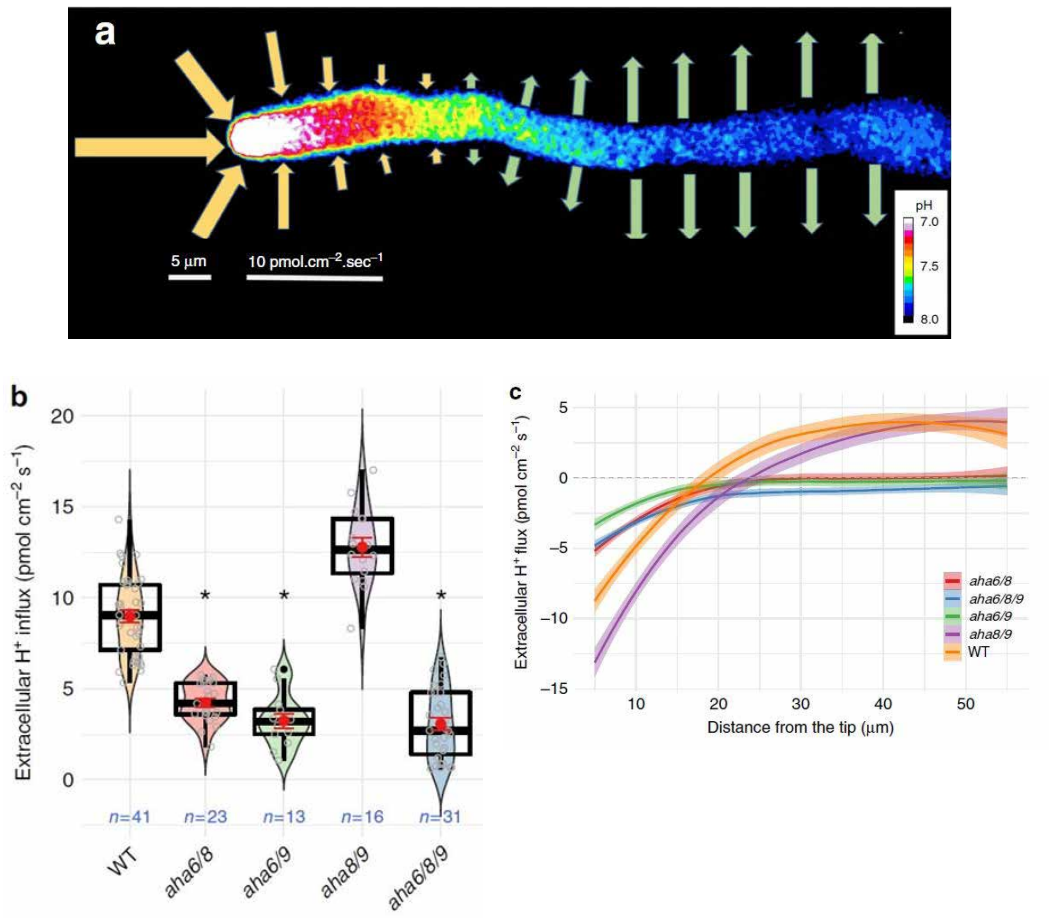

Note. The pollen tube was measured by NMT and its transmembrane H^+ flow was detected. The H^+ flow results could characterize the activity of AHA. The growth rate of all mutant combinations lacking AHA6 decreased, which was related to the reduction of H^+ absorption at the tip (b), the reduction of stem efflux and the retraction of the boundary point of absorption/efflux to the stem (c), especially in the triple mutant. The wild-type pollen tube showed that the absorption of H^+ at the top reversed to the outer row (c) at about 15-20 µm from the top, while almost all the mutant combinations lacking AHA6 did not follow the H^+ outer row of the pollen tube. Although aha8/9 shows a reversal point (c) more than 20 µm from the tip, the absorption of the tip and the outer row along the handle are similar to those of the wild type.

Scientific research combination point of active oxygen and non-invasive micro-test technology (NMT)

I Summary

1. Quantitatively detect the transmembrane H_2O_2 transport rate of living cells and tissues, carry out ROS signal research, and verify the functions of PIP (aquaporin gene)

II Application cases

1. *Nature Commun*: Molecular Mechanism of Improving Callus Culture Ability of Indica Rice

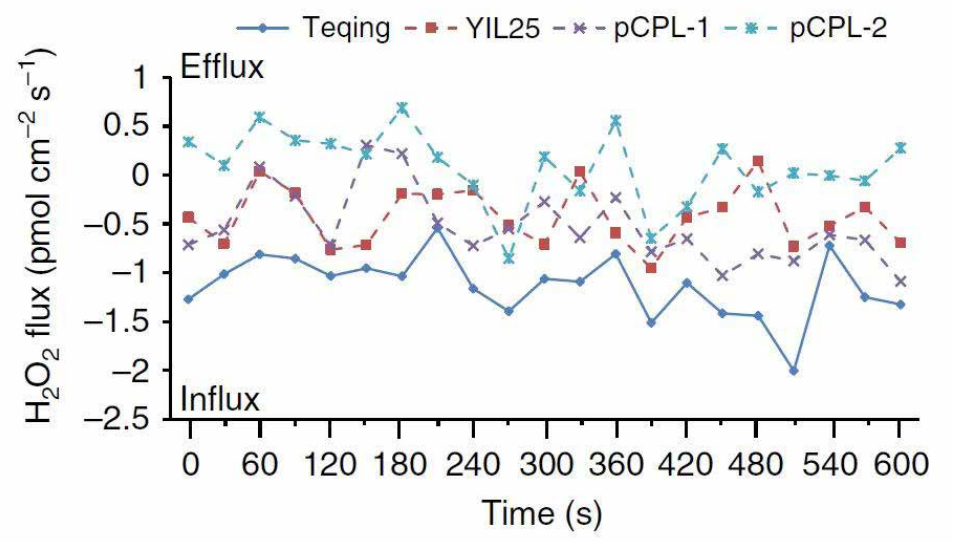

Note. The H2O2 flux between cells of rice calli was measured by using the nondestructive micro-measurement technique (NMT). The intracellular H_2O_2 in YIL25 and pCPL callus was significantly outflow, while the extracellular H_2O_2 in Teqing callus was significantly inflow, indicating that H_2O_2 was discharged from YIL25 or pCPL cells to reduce cell damage.

2. *Plant Cell*: NMT found that ABA and H_2S promote H_2O_2 influx in guard cells, providing evidence for the regulation of ABA-induced stomatal closure by H_2S sulfhydrylation post-translational modification

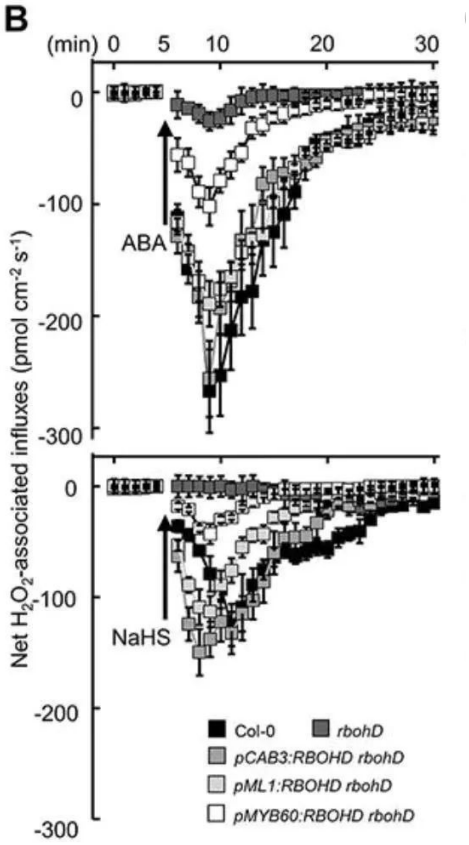

Note. Under ABA or NaHS treatment, *pCAB3: RBOHD rbohD* guard cells found obvious H_2O_2 absorption, while in *rbohD* mutant, small H_2O_2 absorption was detected (Fig. 1B). These results showed that the activity of RBOHD in epidermal and mesophyll cells contributed to the induction of ROS by ABA in guard cells, leading to stomatal closure.

3. *Plant Biotechnol J*: AKR2A coordinates IAA and H2O2 accumulation to control cotton fiber elongation

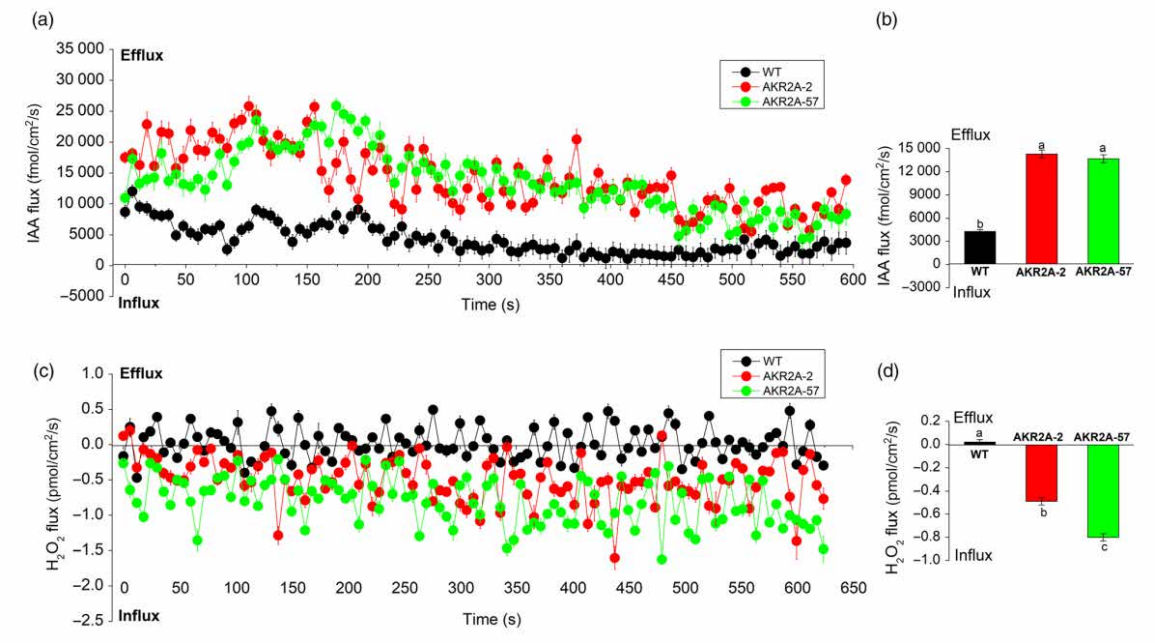

Note. The IAA flow rate of cotton fiber was measured using the non-invasive micro-measurement technology. The IAA in WT was efflux, while the IAA efflux rate of AKR2A-OE was significantly higher than that of WT. The average efflux rate of H_2O_2 in WT is 0.02; The average absorption rates of AKR2A-2 and AKR2A-57 were 0.49 and 0.80 respectively. Compared with WT, the IAA efflux rate and H2O2 absorption rate of AKR2A-OE increased significantly during fiber elongation.

The scientific research combination point of guard cell and non-invasive micro-test technology (NMT)

I Summary

1. Used to quantitatively detect the transmembrane Ca^{2+} signal of guard cells during stomatal movement, and verify the functions of CNGC, OSCA, etc

2. It is used to quantitatively detect the pH change process of guard cells during stomatal movement, i.e., the transmembrane transport rate of H^+, and verify the functions of AHA, OSA, PMA, etc

3. It is used to quantitatively detect the transmembrane transport rate of K^+, Cl^- and NO_3 involved in the regulation of guard cell volume/osmotic pressure in the process of stomatal transport, and verify the functions of GORK, SLAC, etc

4. It is used to quantitatively detect ROS (H_2O_2) transmembrane transport rate of guard cells during stomatal movement, and verify functions such as PIP

二、应用案例

1. *Nature*：Non-destructive "electrophysiological" calcium flow provides key evidence for the identification of stomatal immune calcium channel OSCA1.3

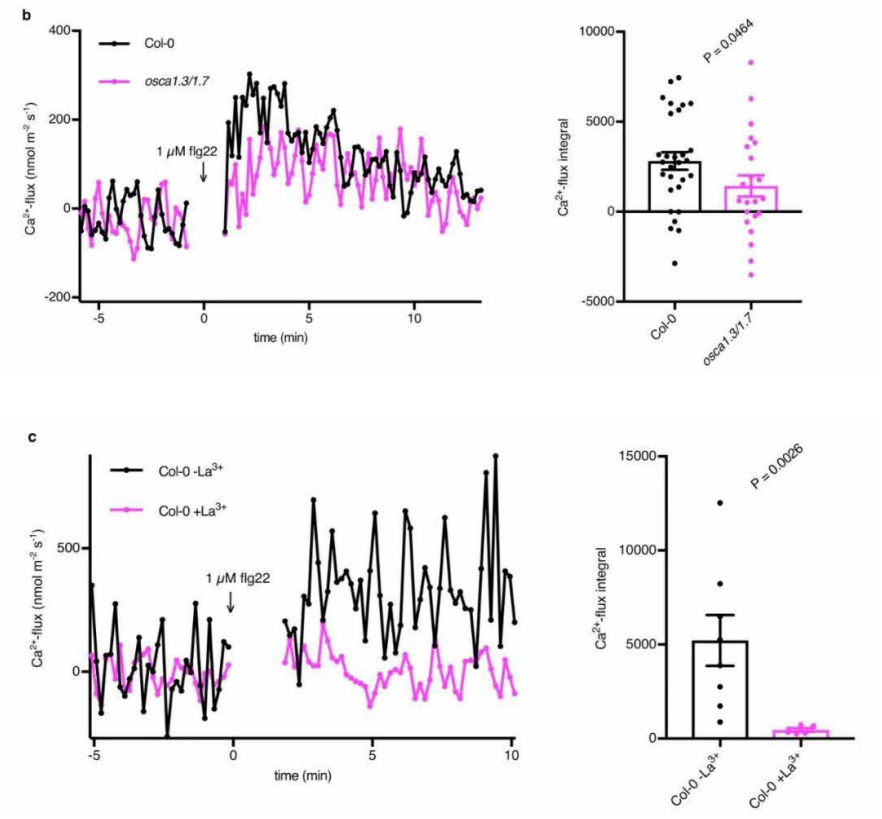

Note. The net Ca^{2+} flow rate of guard cells of Col-0 and *osca1.3/1.7* was measured using non-invasive micro-measurement technology. The results showed that compared with Col-0, the absorption rate of Ca^{2+} in 7 minutes after adding flg22 decreased in *osca1.3/1.7* (b). The Ca^{2+} absorption rate of Col-0 guard cells with or without lanthanum chloride pretreatment was detected. It was found that the Ca^{2+} absorption was significantly blocked within 8 minutes after adding flg22 after lanthanum chloride treatment (c).

2. PNAS：NMT provides key evidence to reveal that the evolution of chloroplast retrograde signals has promoted the adaptation of green plants to land

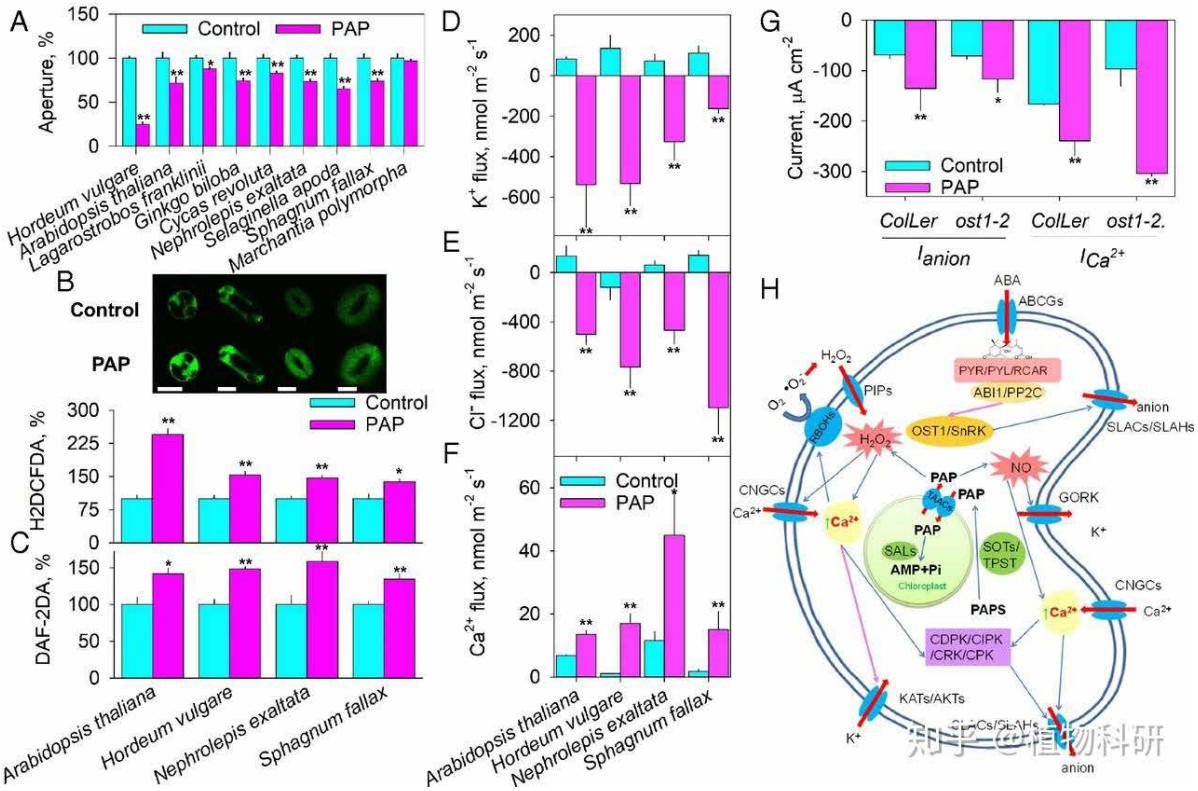

Note: The addition of PAP led to the significant closure of plant stomata. The degree of conservative evolution of PAP on the ion transport of guard cells was studied using NMT. The outflow of K^+ and Cl^- was accompanied by an average increase of 4.3 times of Ca^{2+} inflow, and the K^+ and Cl^- transmembrane was from the inside to the outside. PCR of Arabidopsis wild-type plant guard cells showed that GORK and SLAC1 were significantly up-regulated by PAP, while KAT2 was significantly down-regulated. The increase of PAP will lead to a significant increase of Ca^{2+} and anions in guard cells.

3. *Plant Physiol*: NMT found that ABA could not induce K^+ excretion and Ca^{2+}uptake of fern/lycopodium guard cells, which showed that ABA was significantly different from gymnosperms/angiosperms

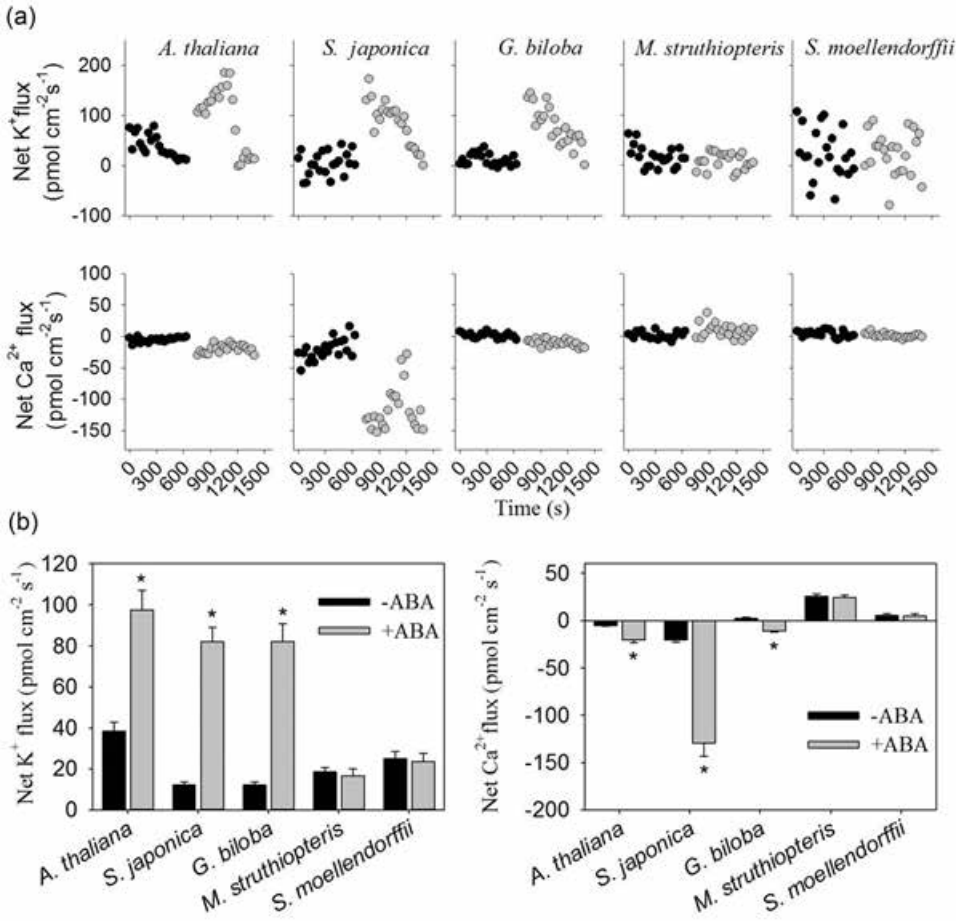

Note. The effect of ABA on the K^+ and Ca^{2+} flow rates of guard cells of five seed plants, including Arabidopsis thaliana, S. japonica, G. biloba, M. striopteris and S. moellendorfii. A. After adding 50 μ The flow rate changes of K^+ and Ca^{2+} were recorded before (black circle) and after (gray circle) M ABA solution. B. Add 50 μ Before and after ABA solution, the K^+ efflux and Ca^{2+} influx on the surface of guard cells of five seed plants changed significantly, while the guard cells of ferns and lycopsids did not change significantly before and after ABA solution was added (black column) (gray column).

NMT Communications

March 2023 Volume 1 Issue 2

Publisher: Non-invasive Micro-test Technology International Alliance
Publisher Address: 19 Research Drive, Suite 6 Amherst, MA 01002

Organizer: Zhongguancun Xuyue Non-invasive Micro-test Technology Industrial Alliance
Editor-in-Chief: Xu Yue and Liu Yunqi
Honorary Editors: Kuang Tingyun,Sergey Shabala, Marshall Porterfield
Address of editorial office: 19 Research Drive, Suite 6 Amherst, MA 01002

Executive Editor: Li Xuefei
Editors: Zhang Zengkai, Gao Hongjian, Li Lei, Ye Bin, Ju Xiaoyu, Ma Yue, Guo Weiwei, Liu Peiqi
Art Editors: Liu Zhaoyi, Wang Yang

International Standard Serial Number (Online): ISSN2834-5363
International Standard Serial Number (Print): ISSN2834-5355
Submission email: yanhan@nmtia.org.cn
Tel: 010-8262 4800

Copyright Notice